

Figure S1A-B

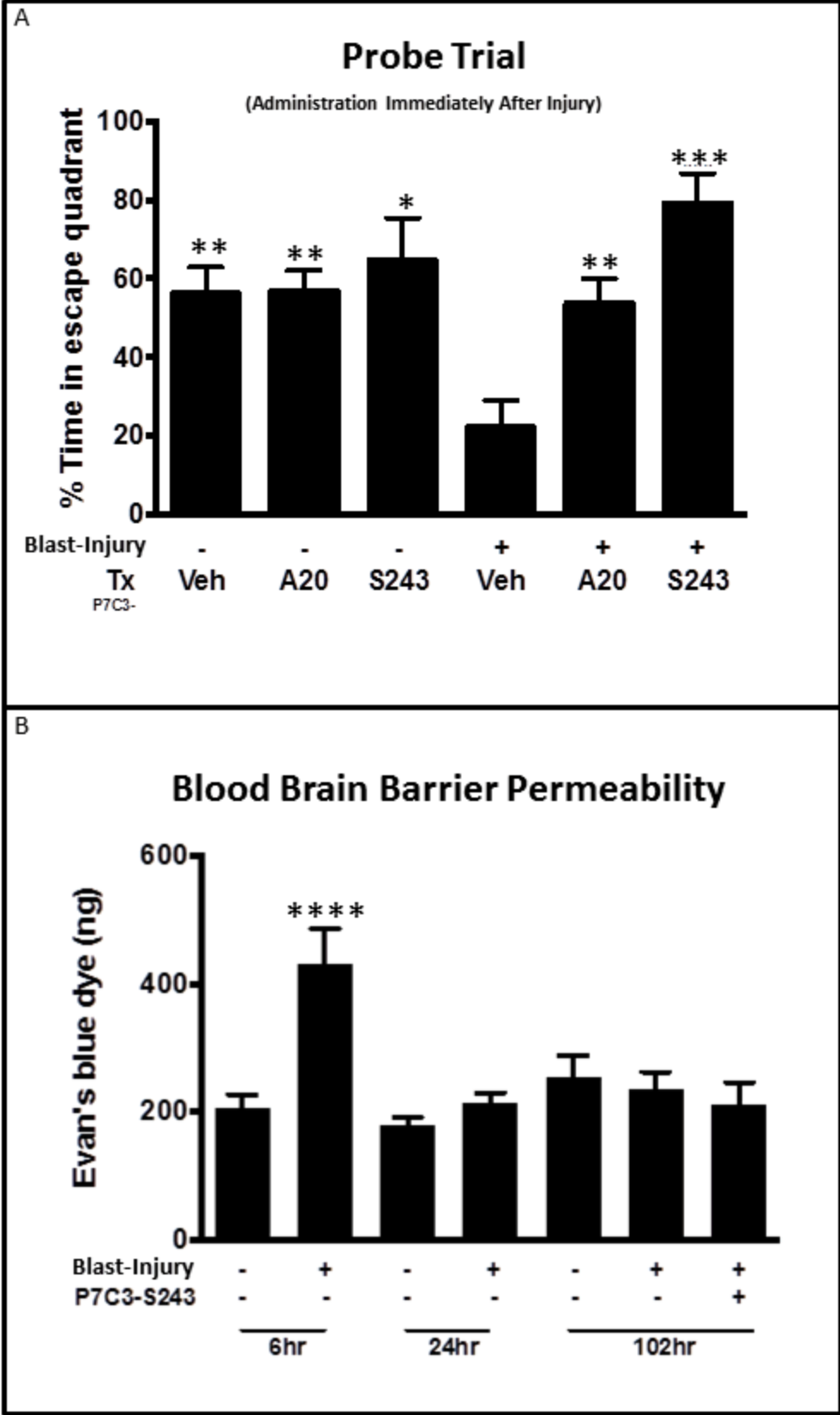


Figure S1C

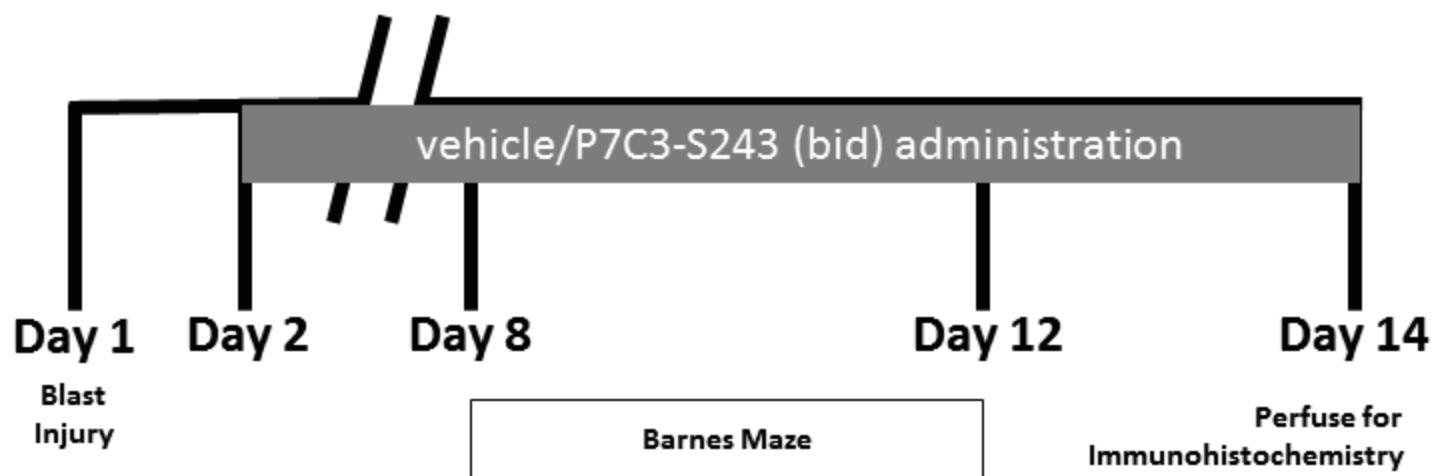


Figure S2A-C

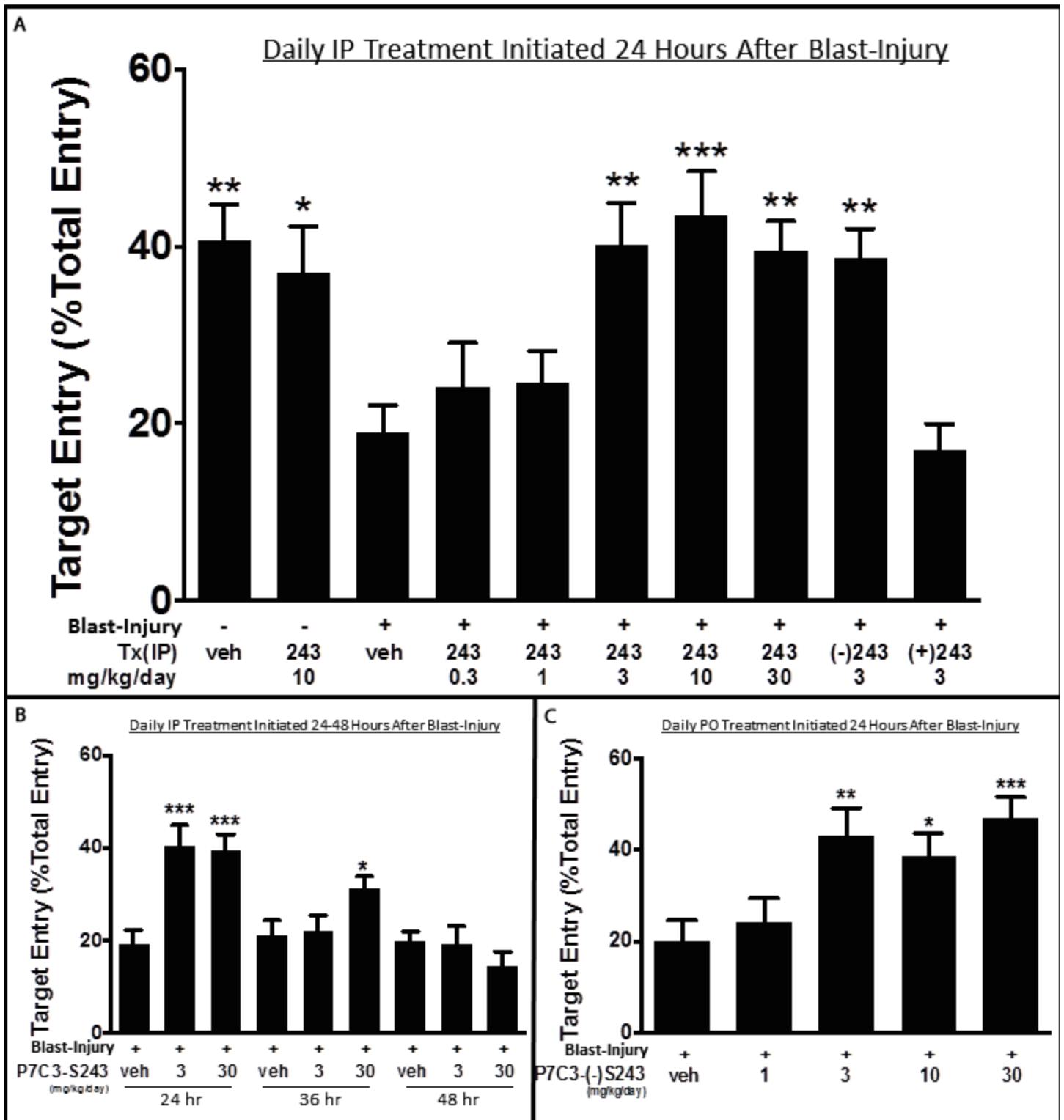


Figure S2D-F

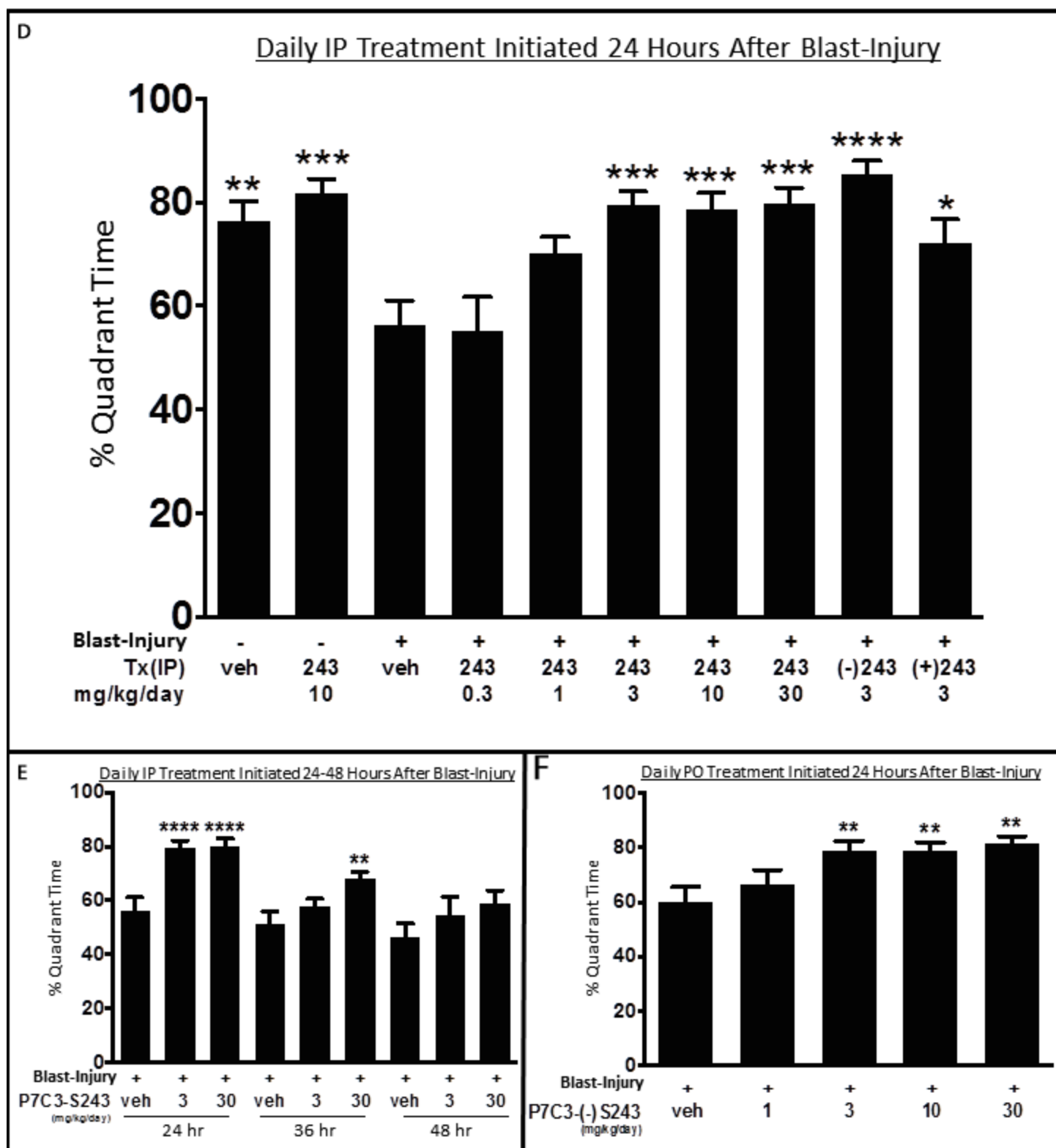


Figure S2G-I

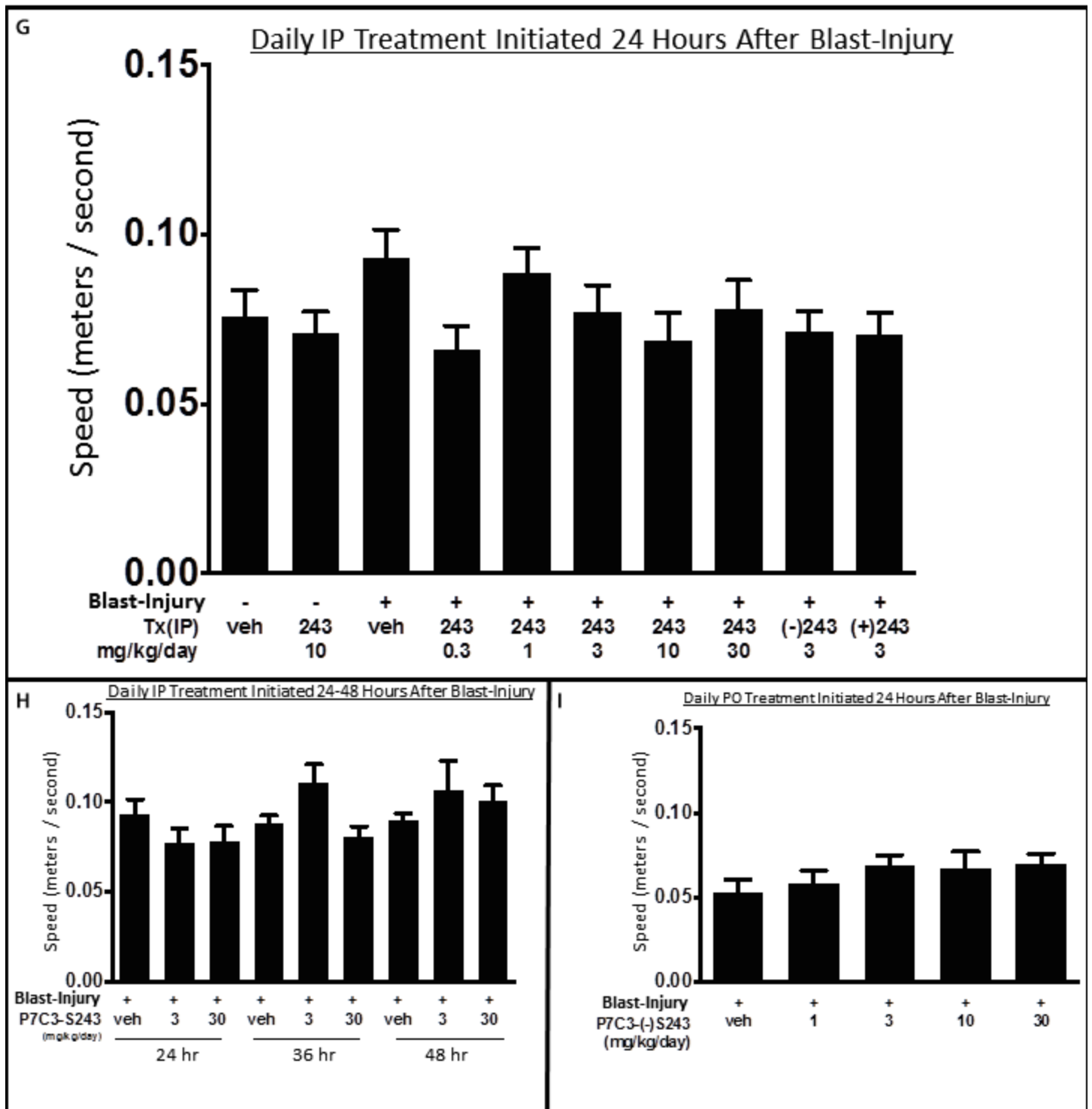


Figure S2J-L

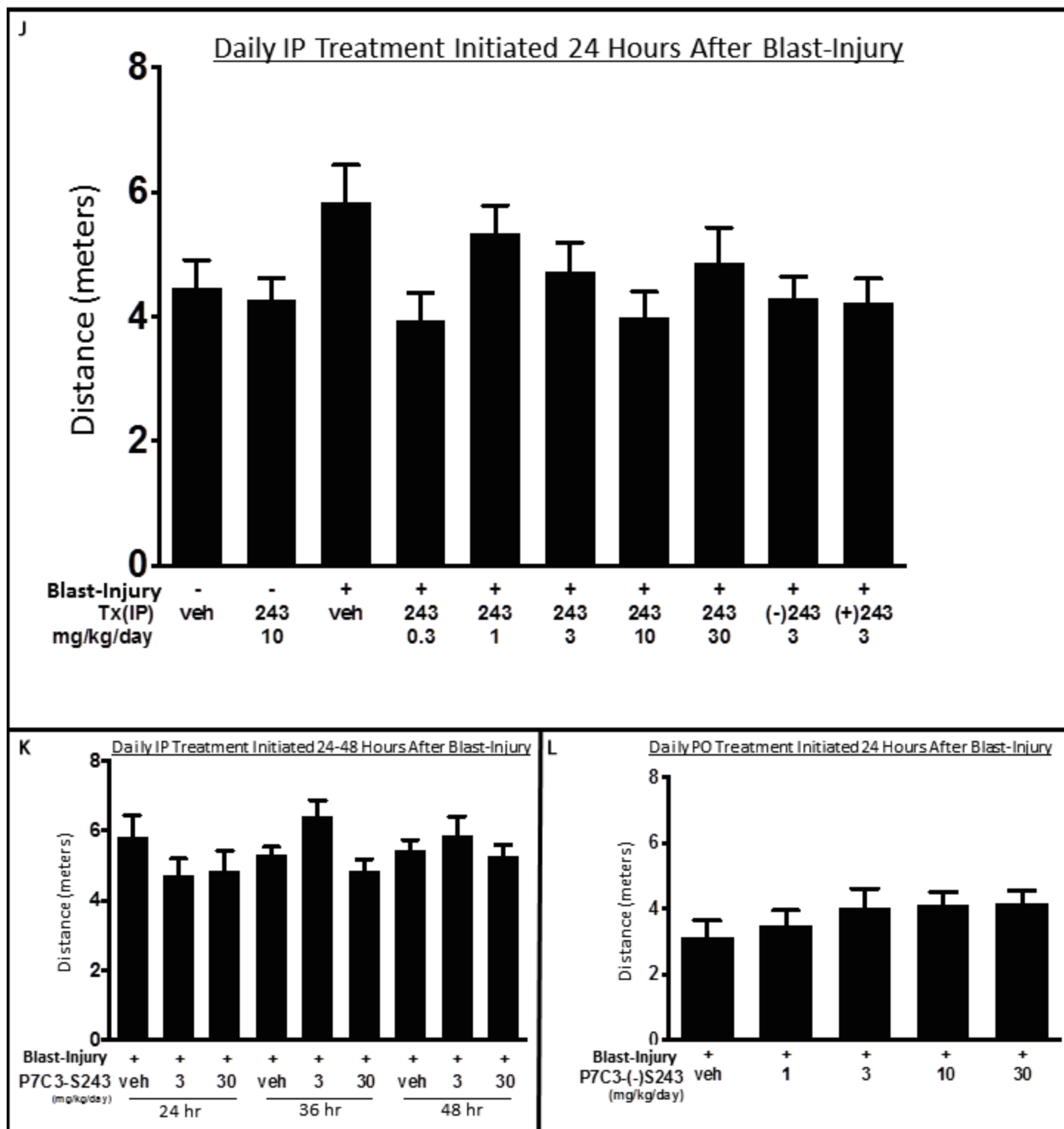


Figure S2M-O

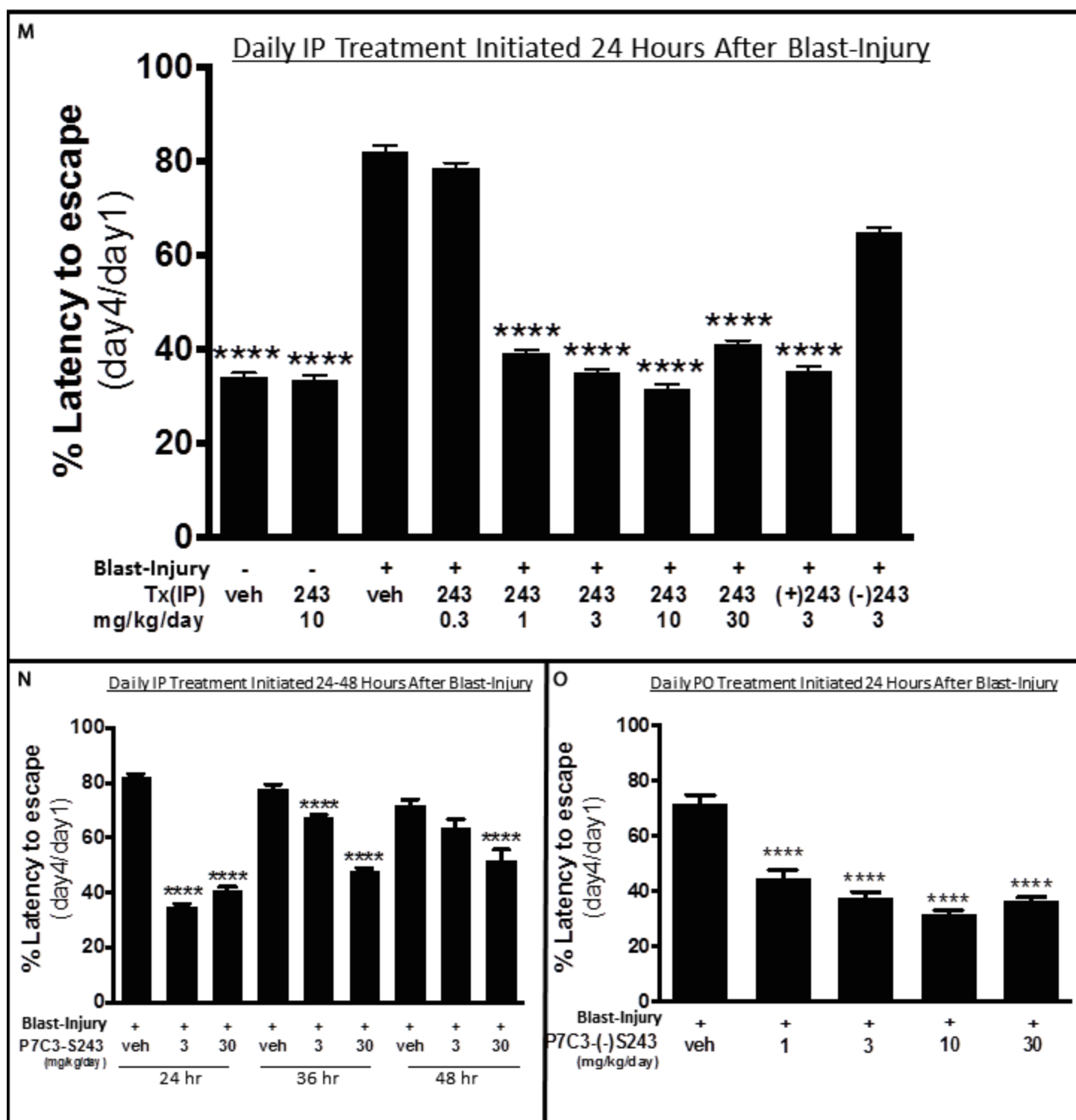


Figure S2P-U

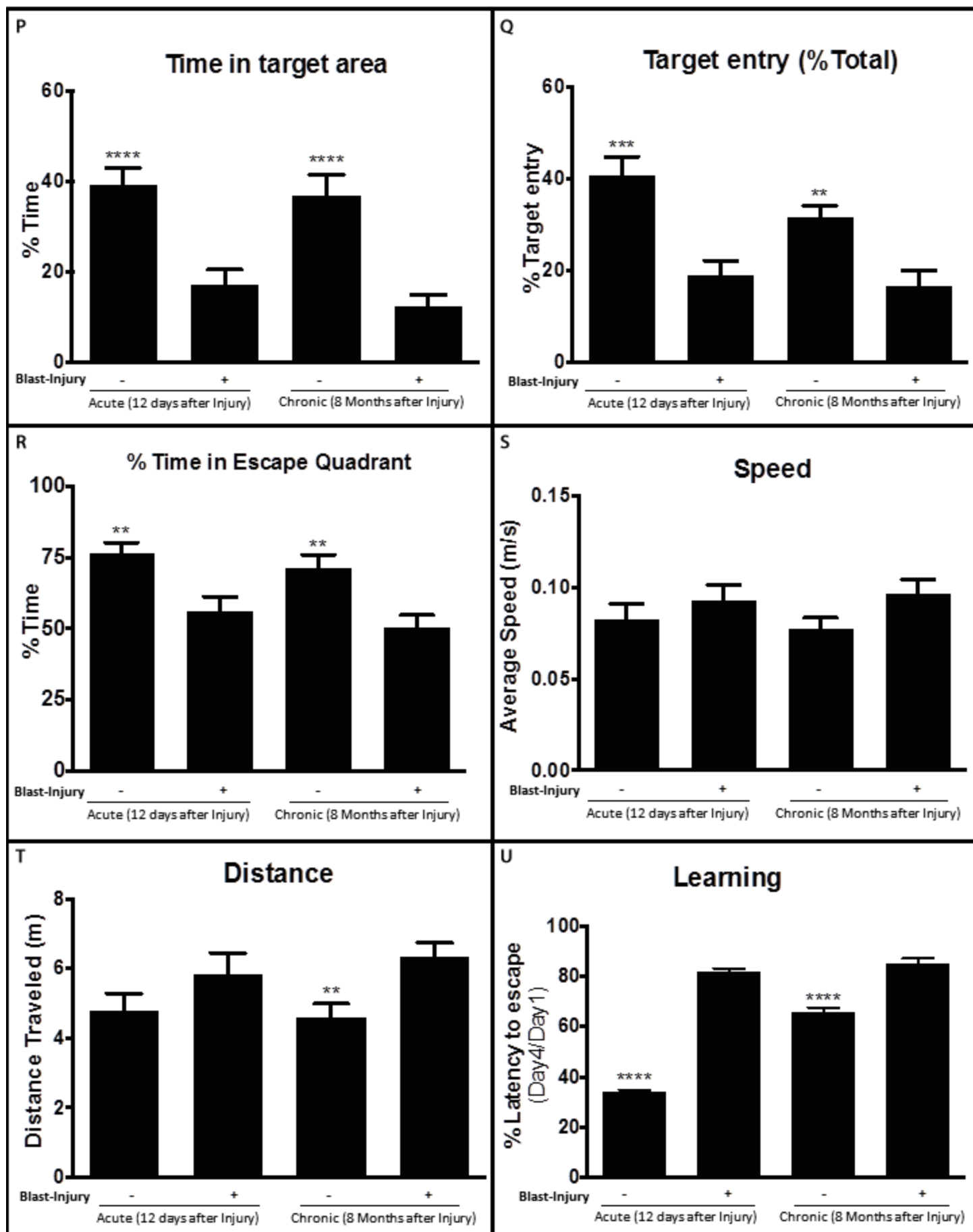


Figure S3A

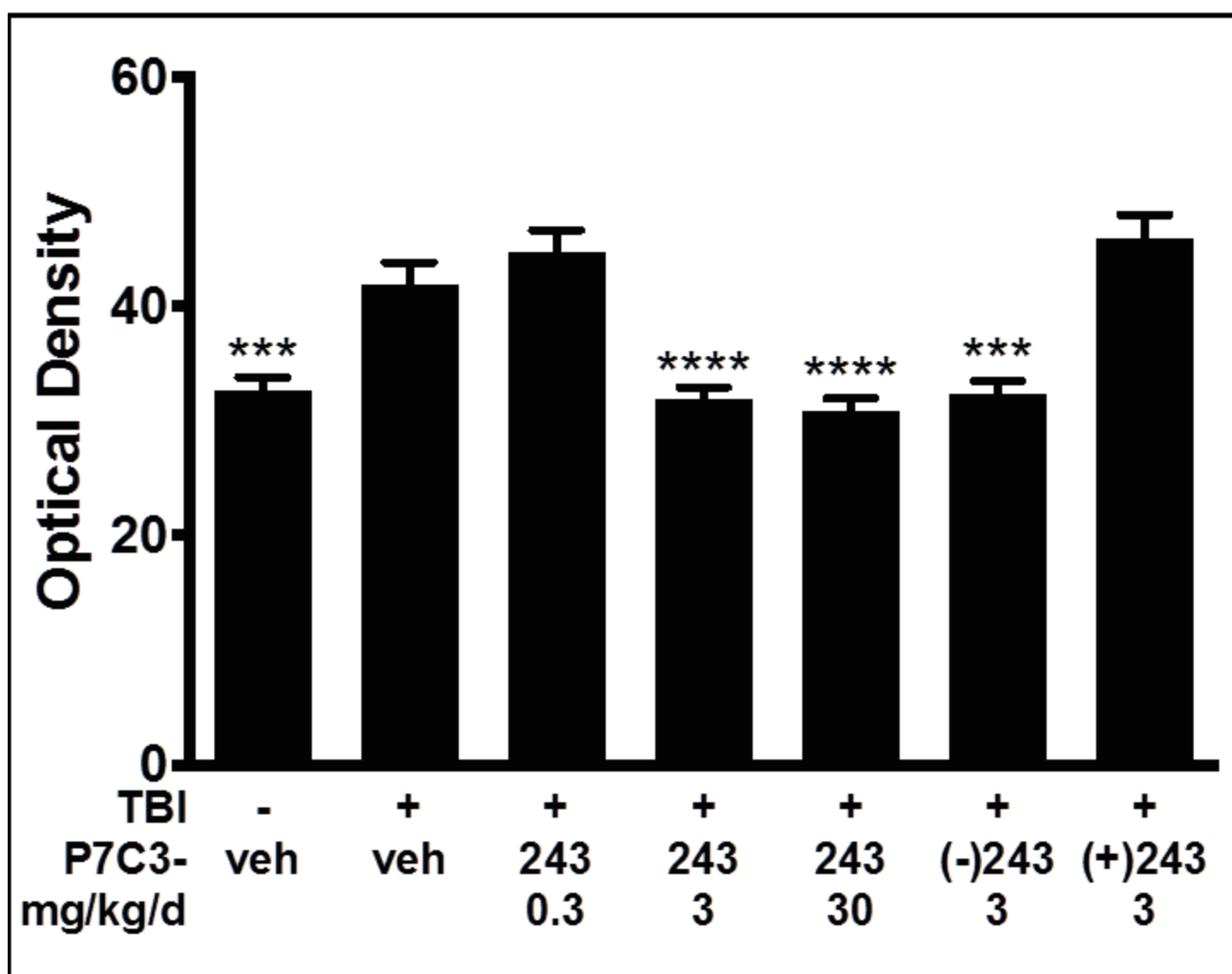


Figure S3B

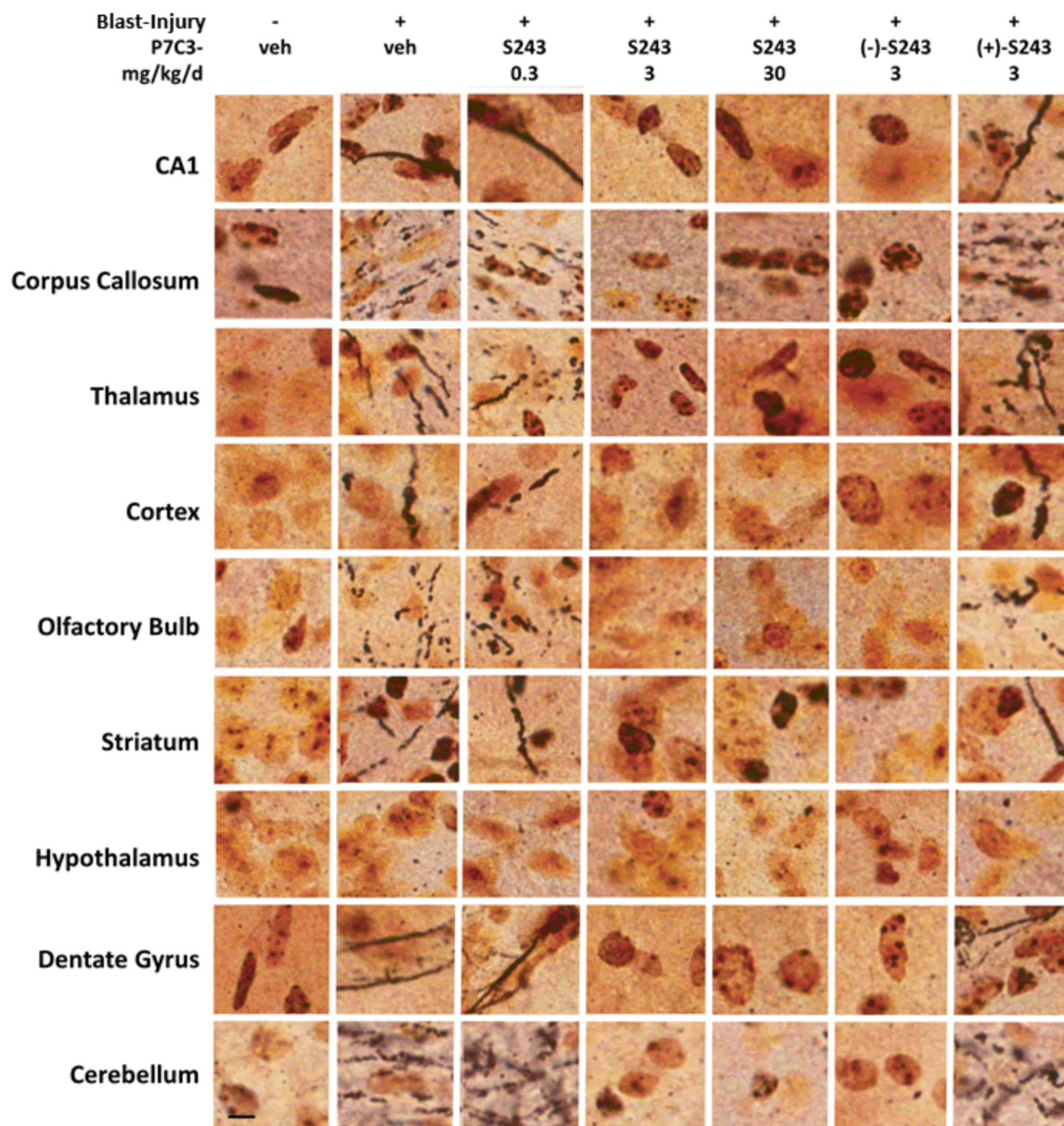


Figure S3C

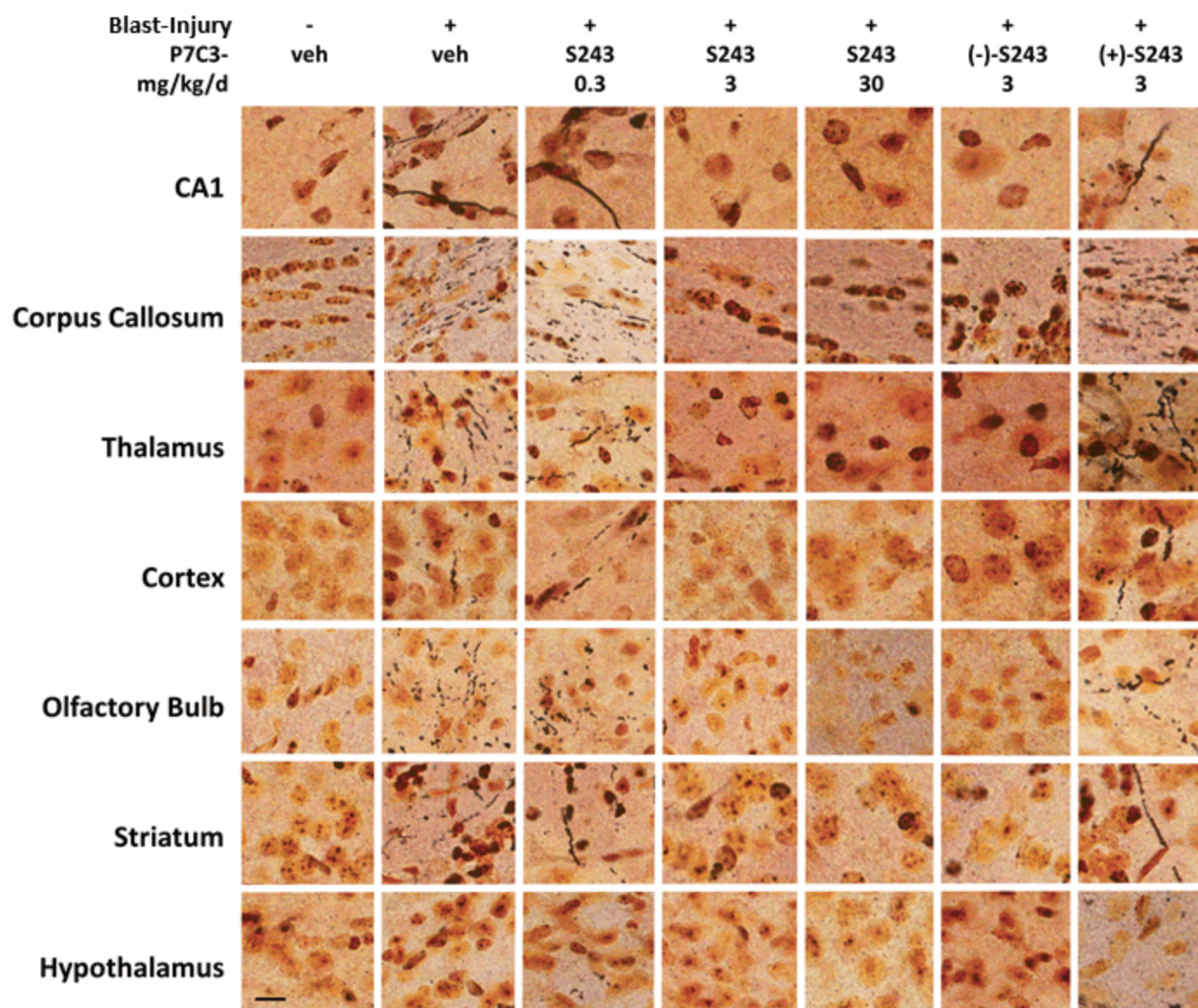


Figure S3D

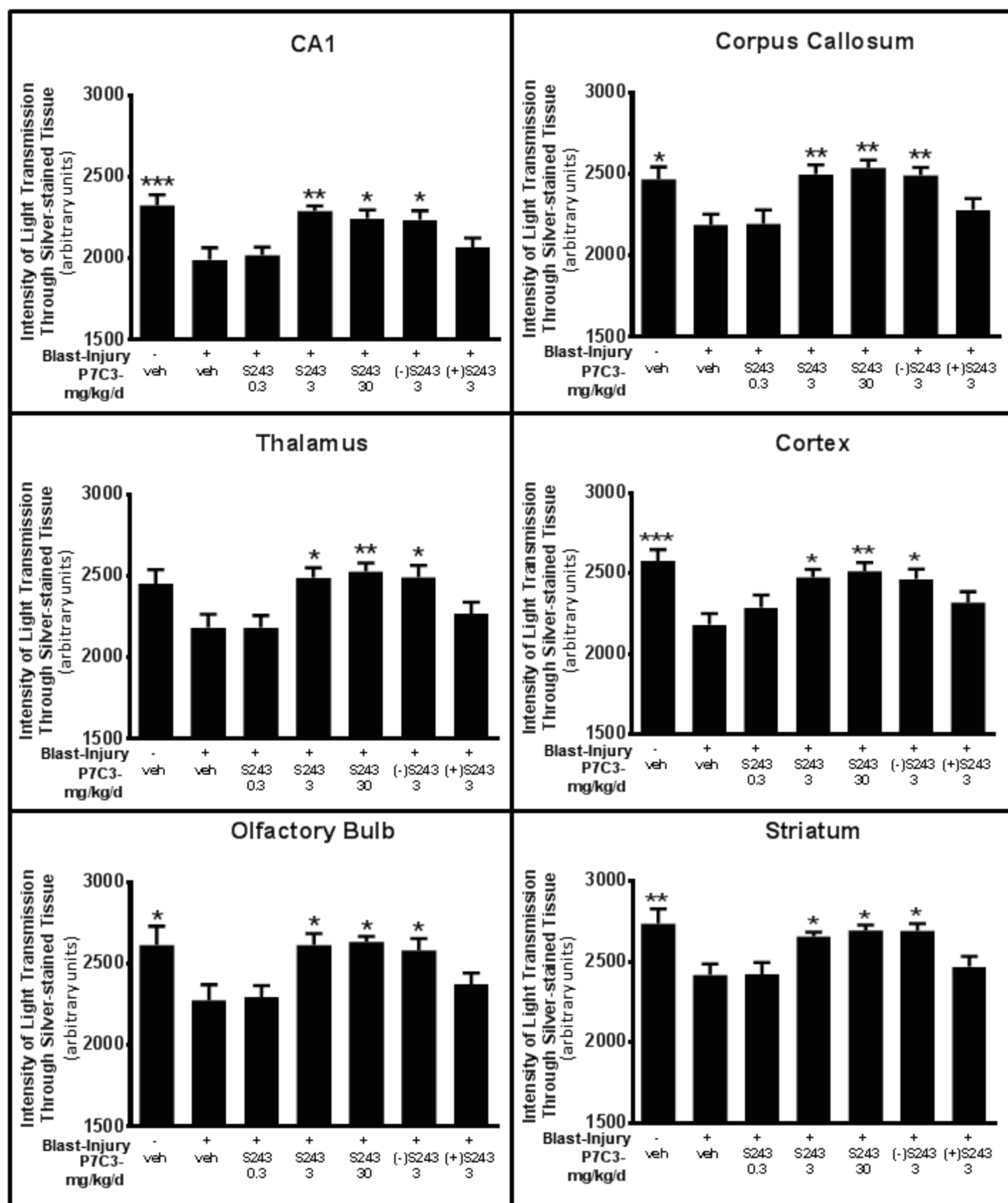


Figure S3E

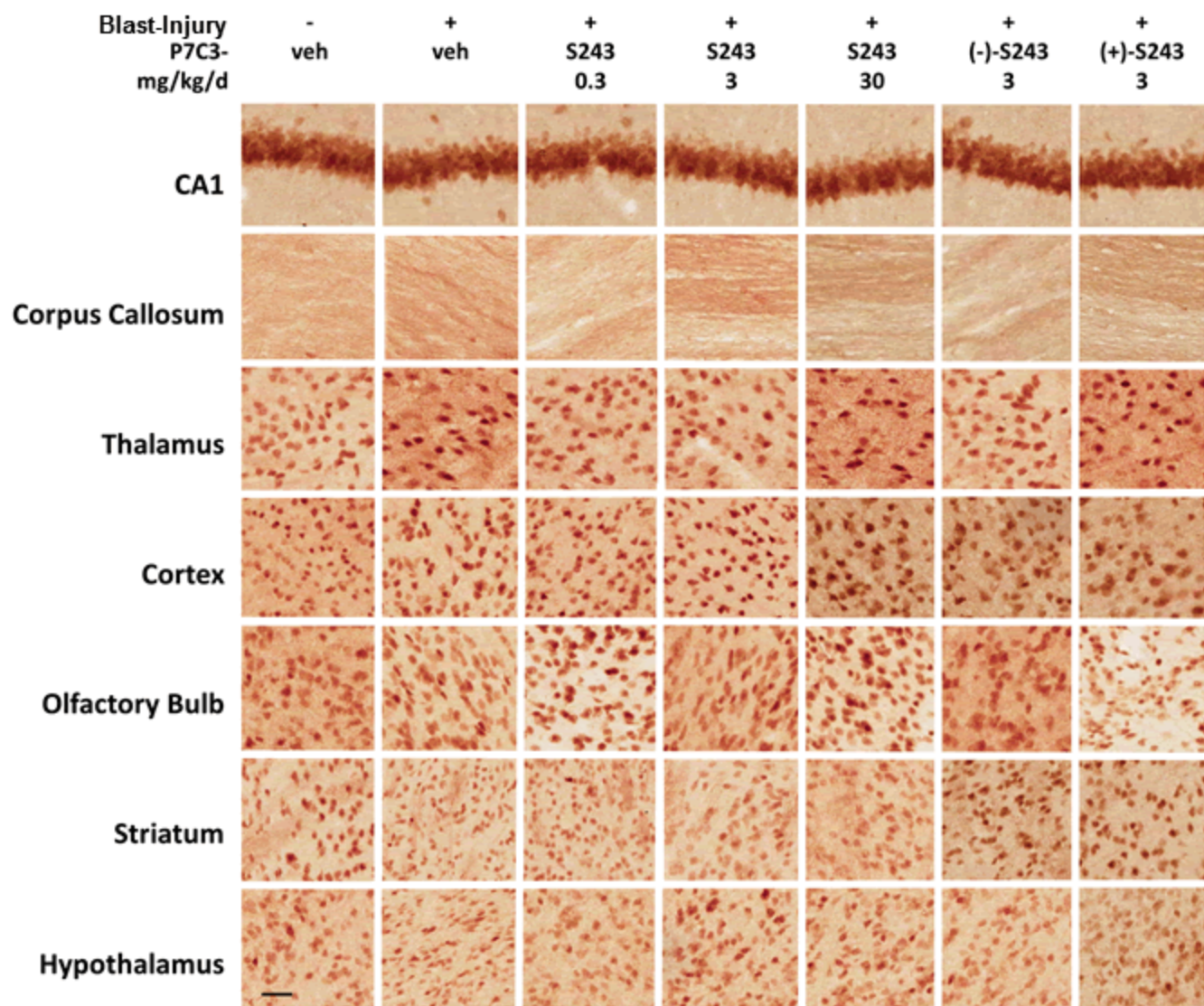


Figure S3F

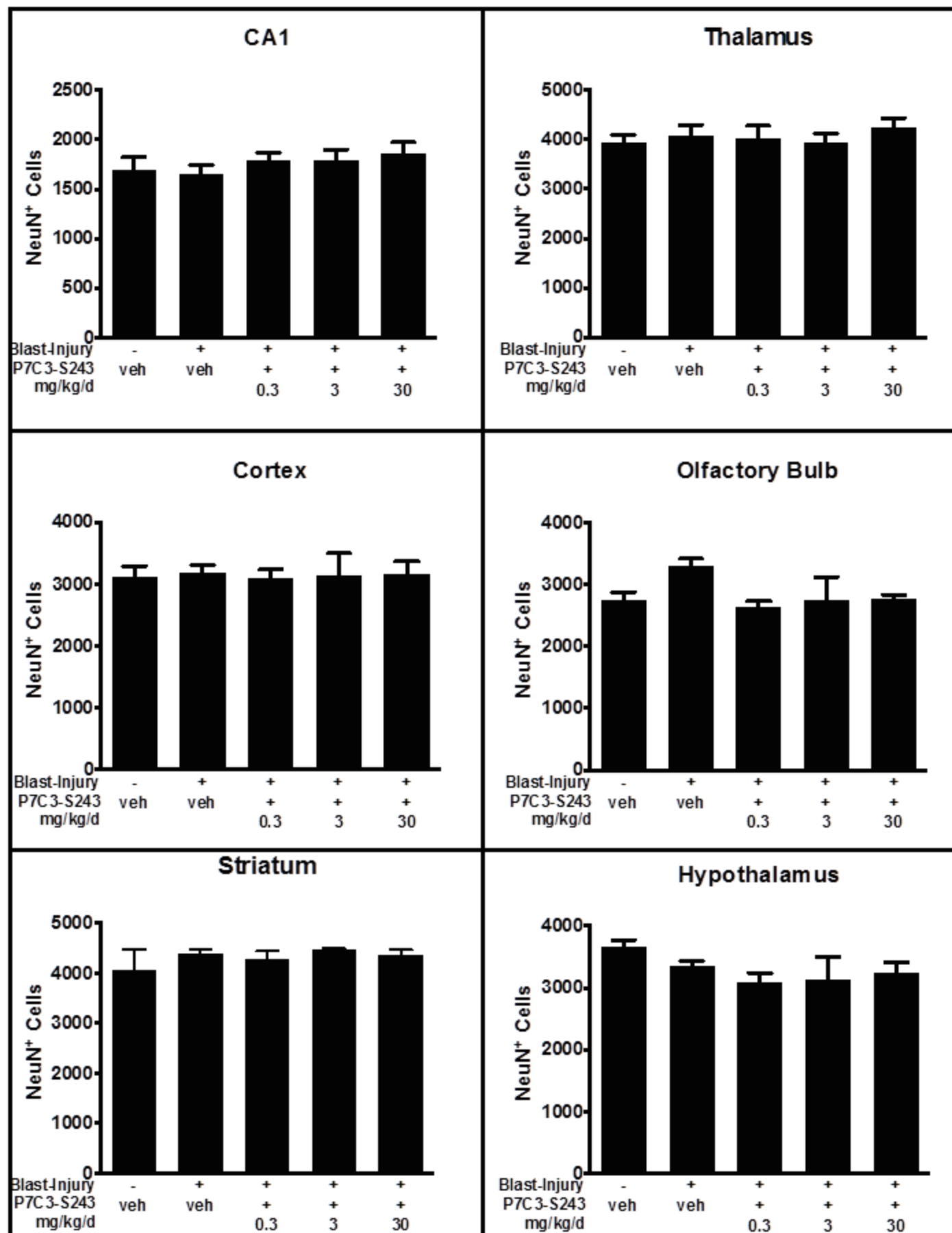


Figure S3G

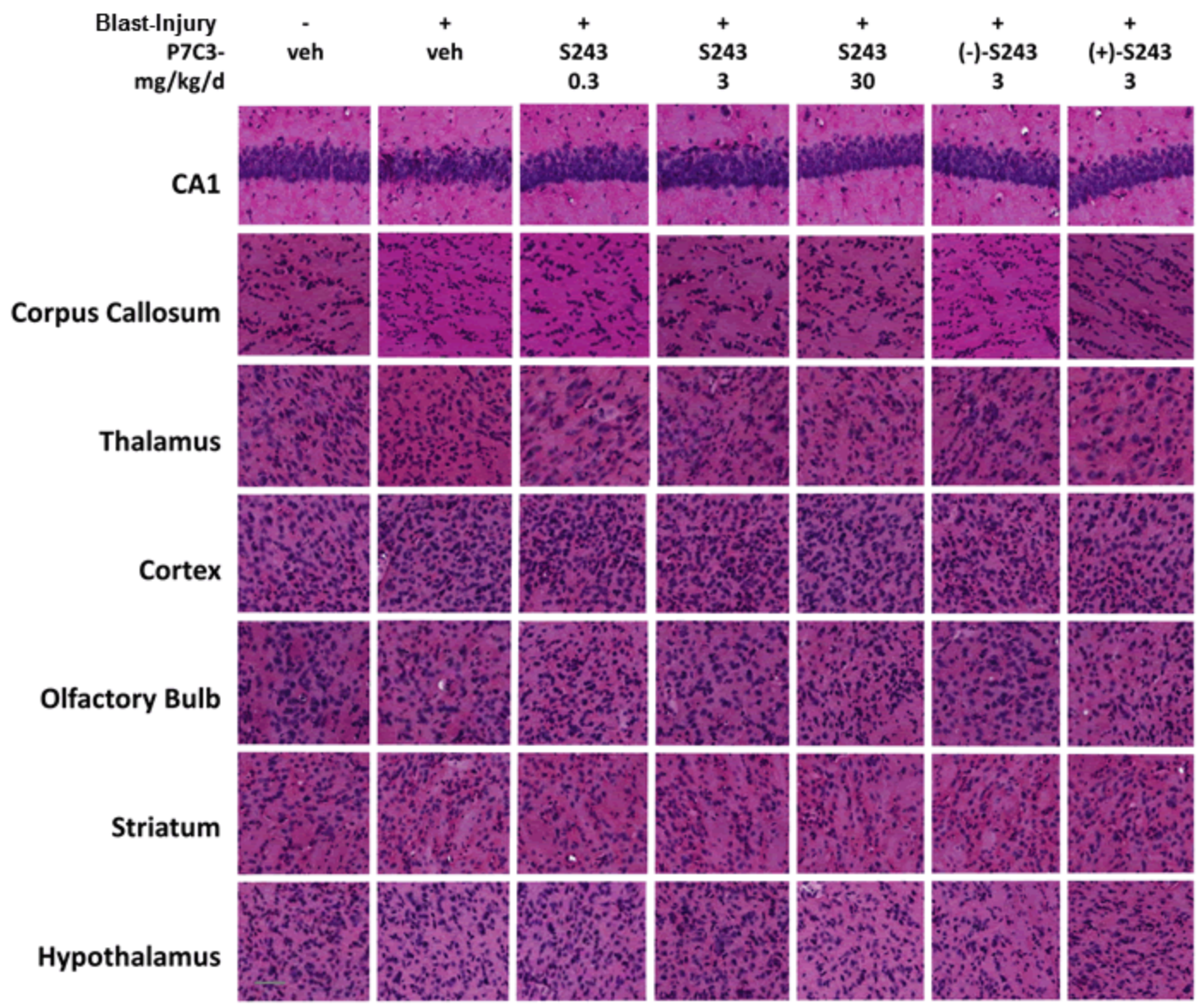


Figure S3H

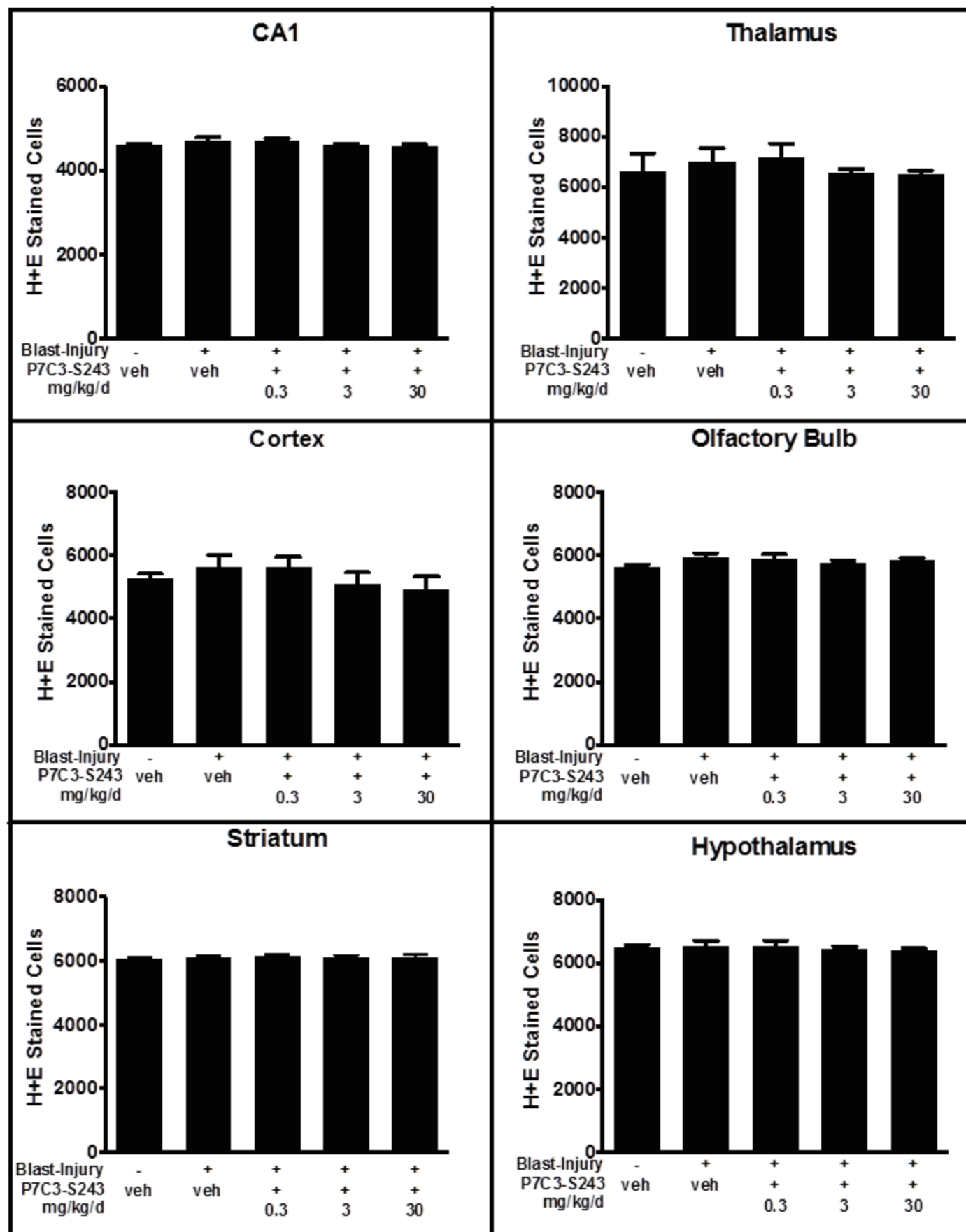


Figure S3I



Figure S4A-C

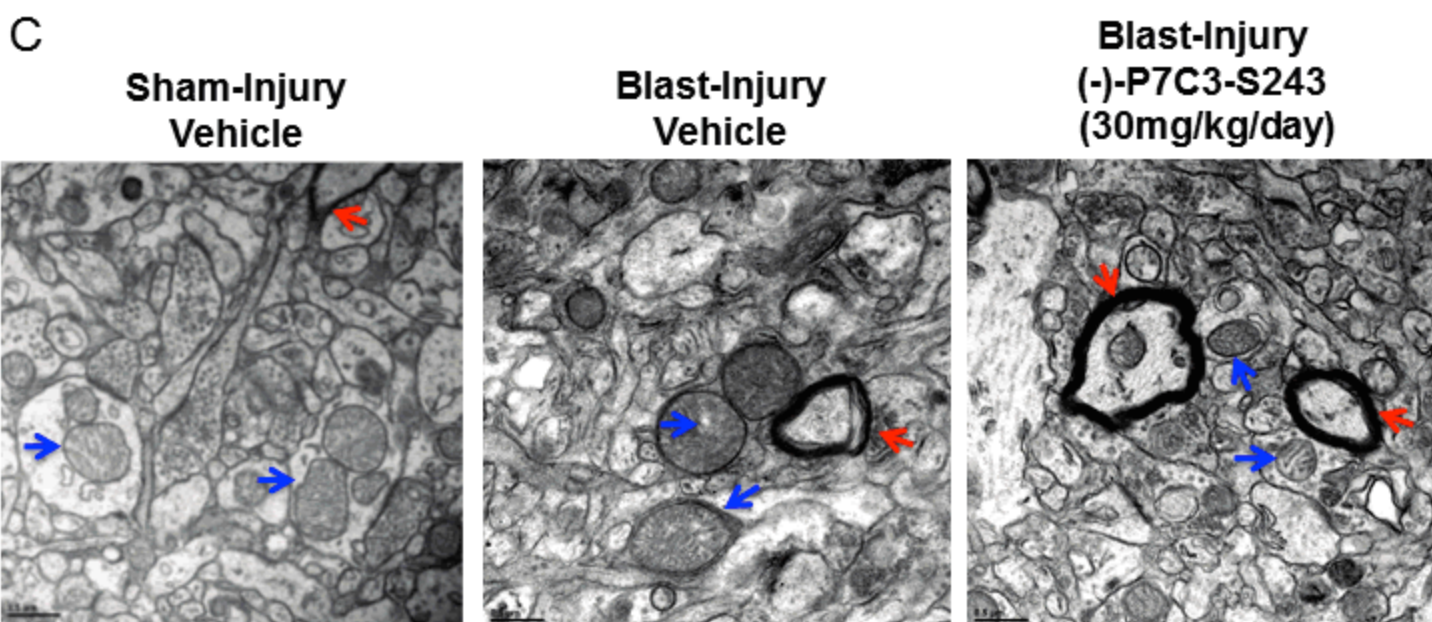
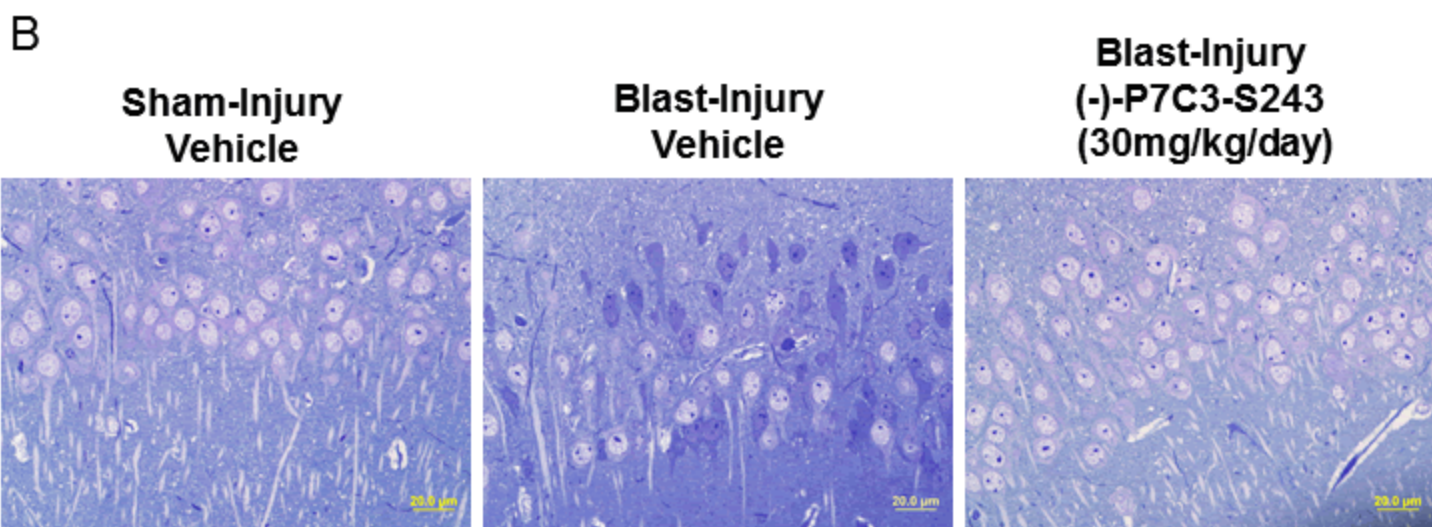
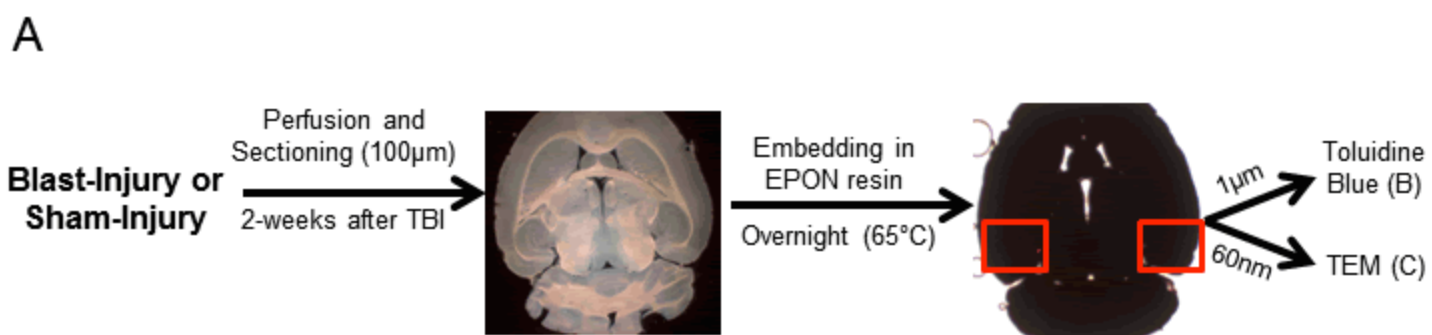


Figure S4D

SHAM-Injury
Vehicle

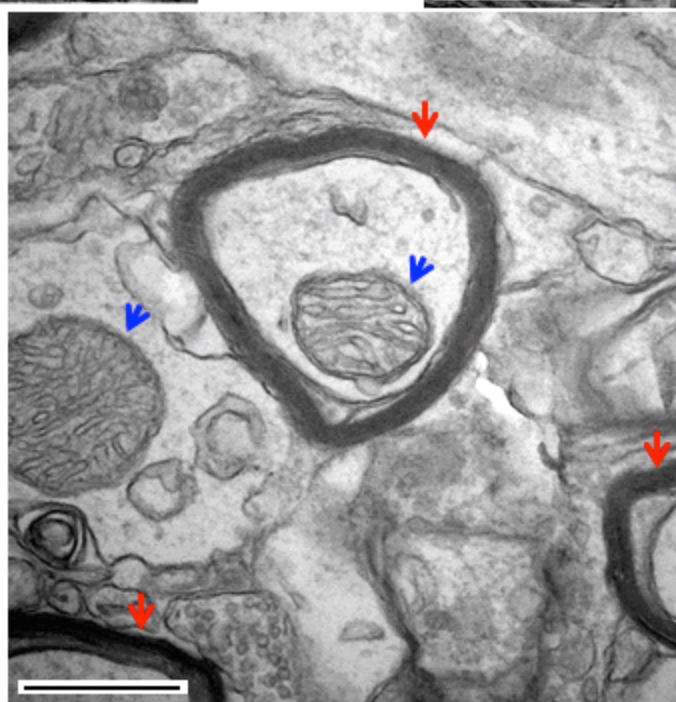
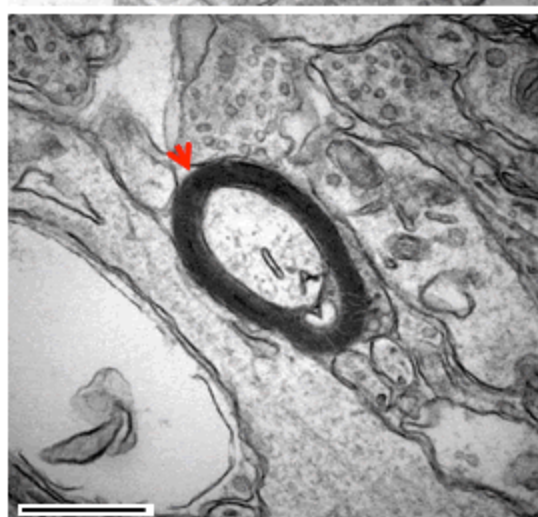
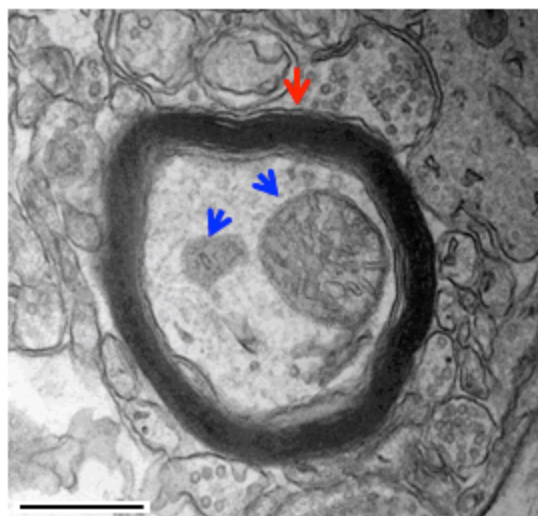
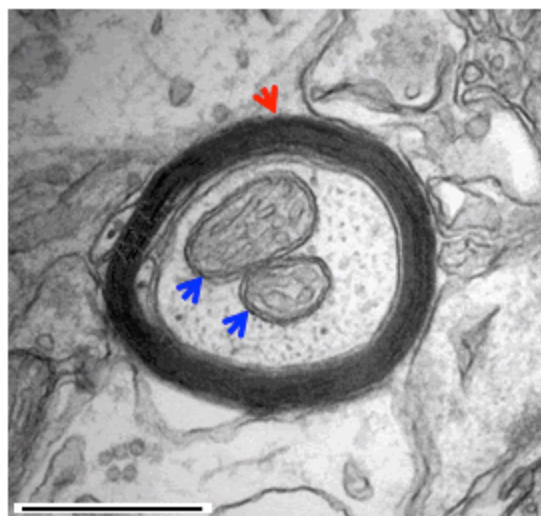


Figure S4E

SHAM-Injury
(-)-P7C3-S243
30 mg/kg/d

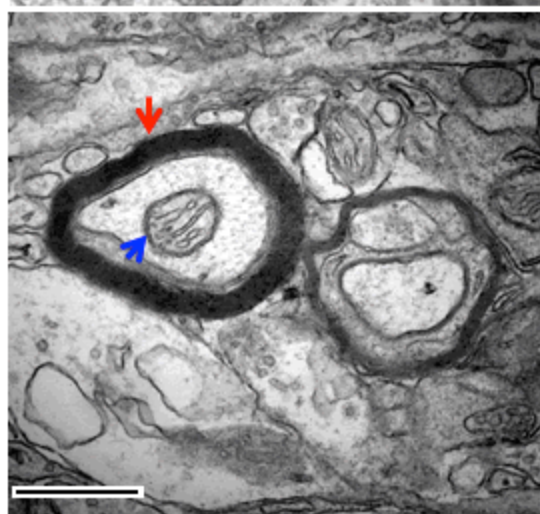
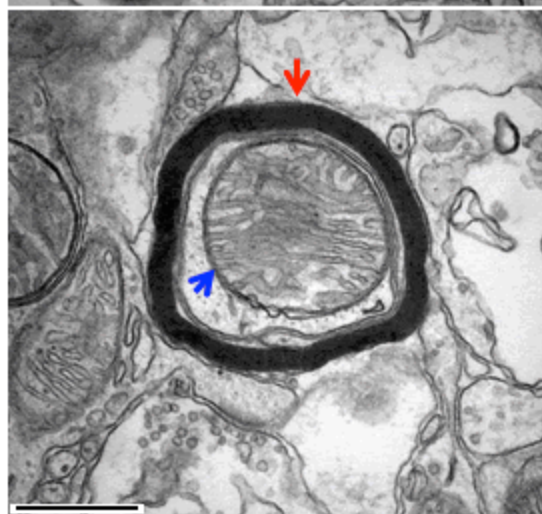
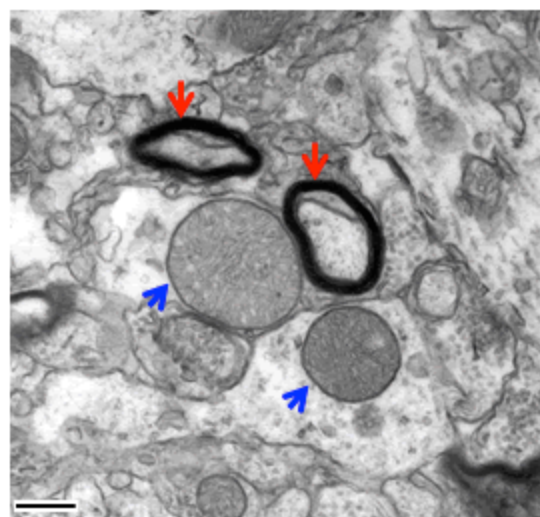
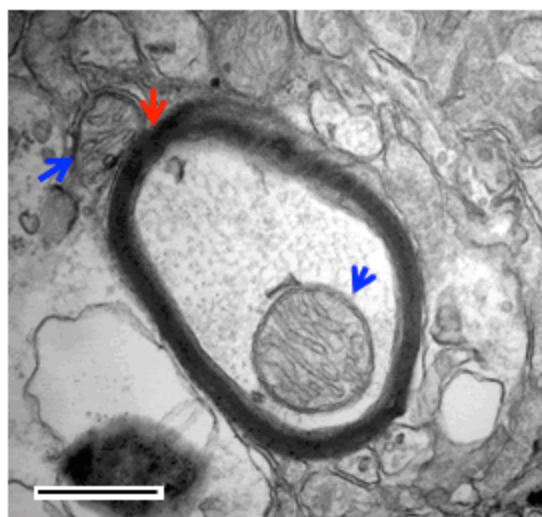


Figure S4F

Blast-Injury
Vehicle

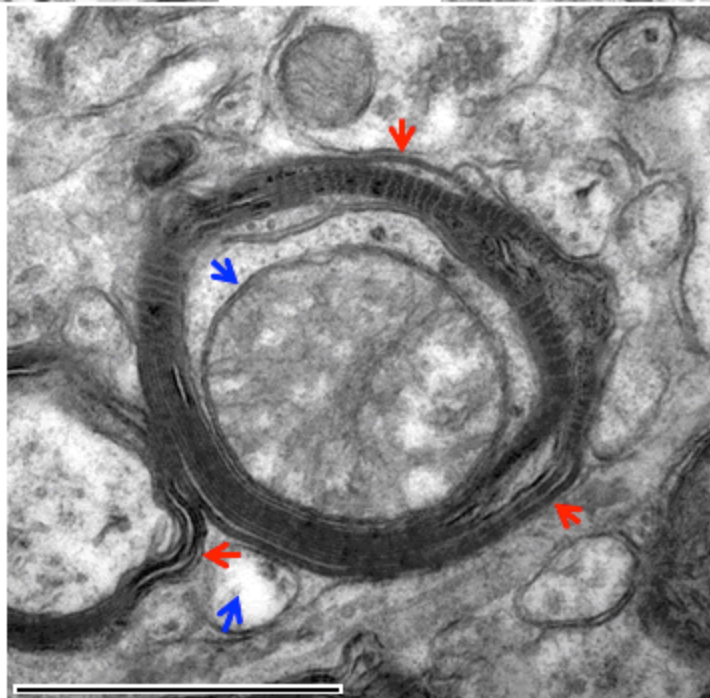
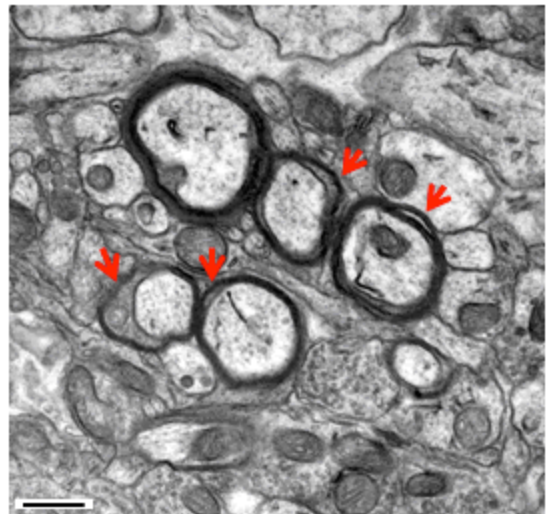
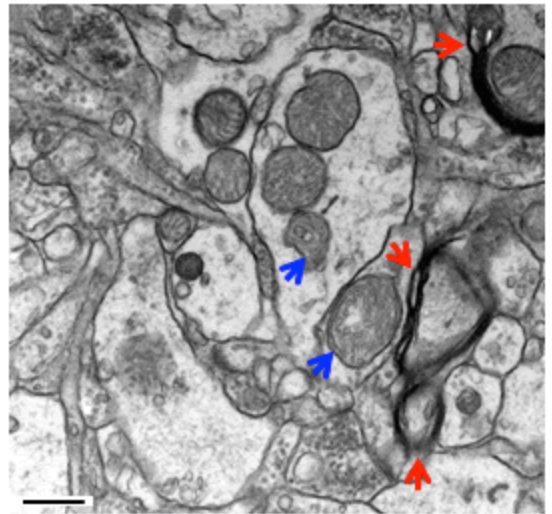
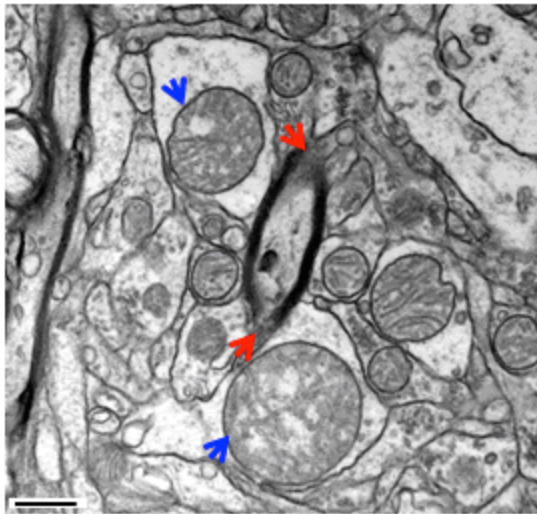


Figure S4G

Blast-Injury
(-)-P7C3-S243
0.3 mg/kg/d

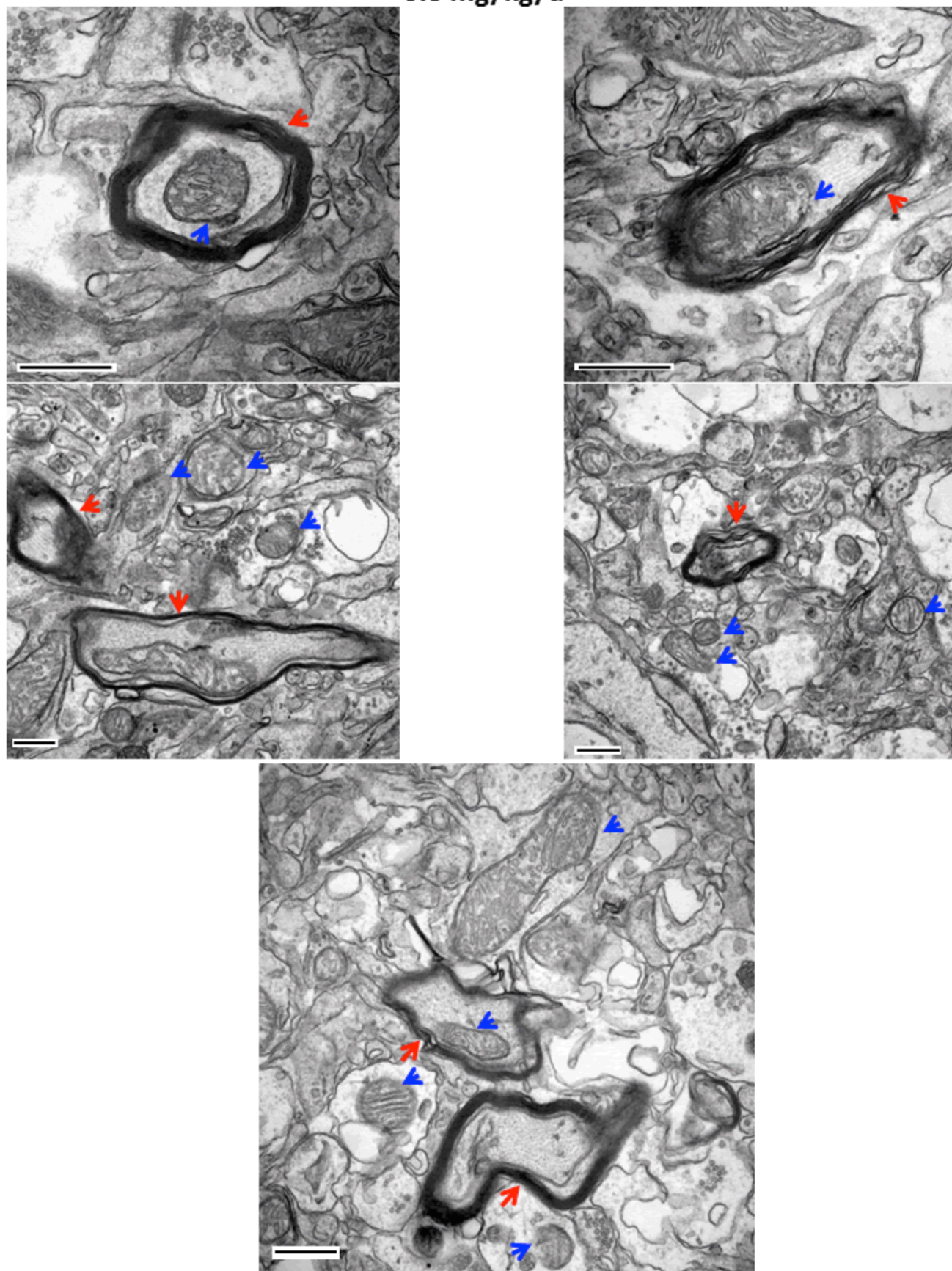


Figure S4H

Blast-Injury
(-)-P7C3-S243
3 mg/kg/d

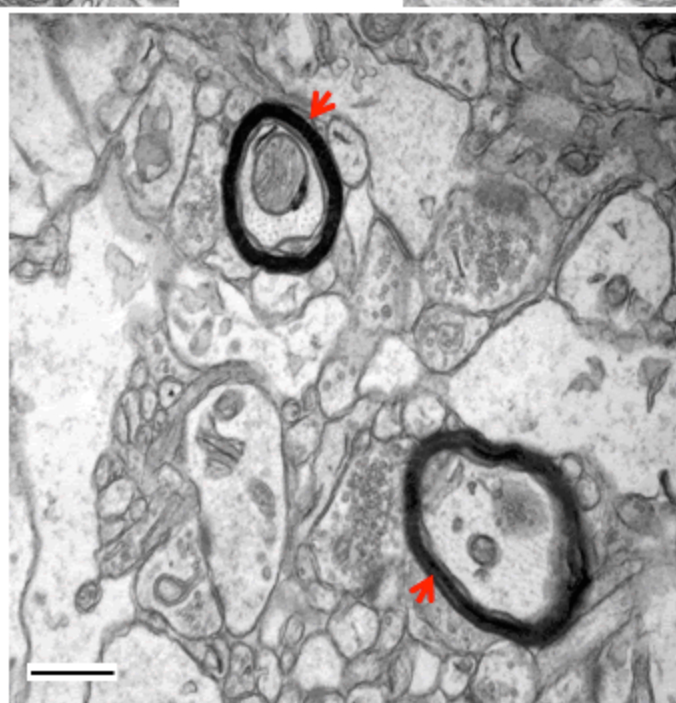
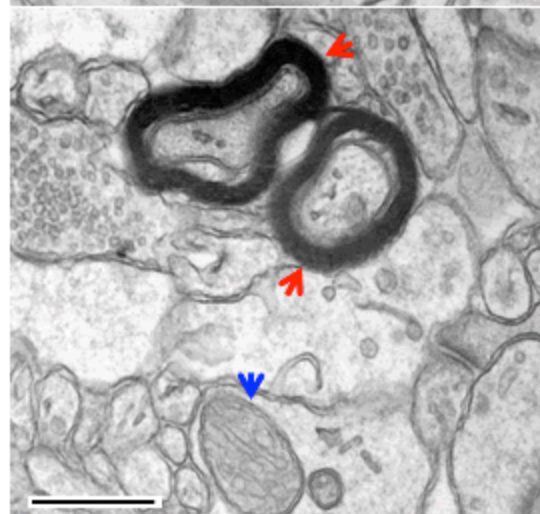
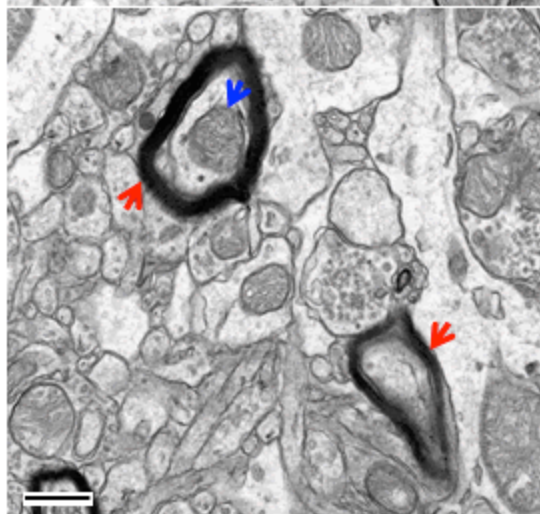
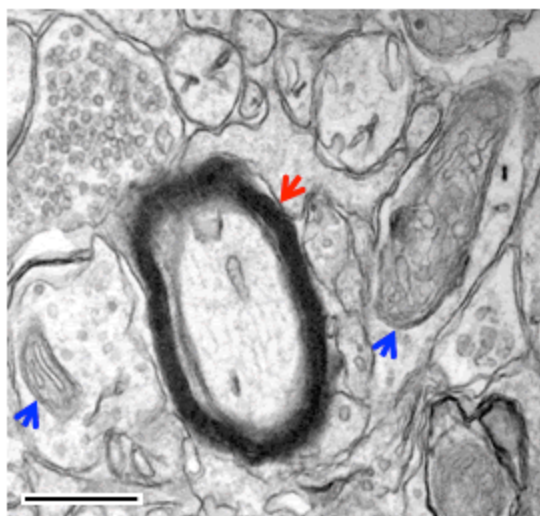


Figure S4I

Blast-Injury
(-)-P7C3-S243
30 mg/kg/d

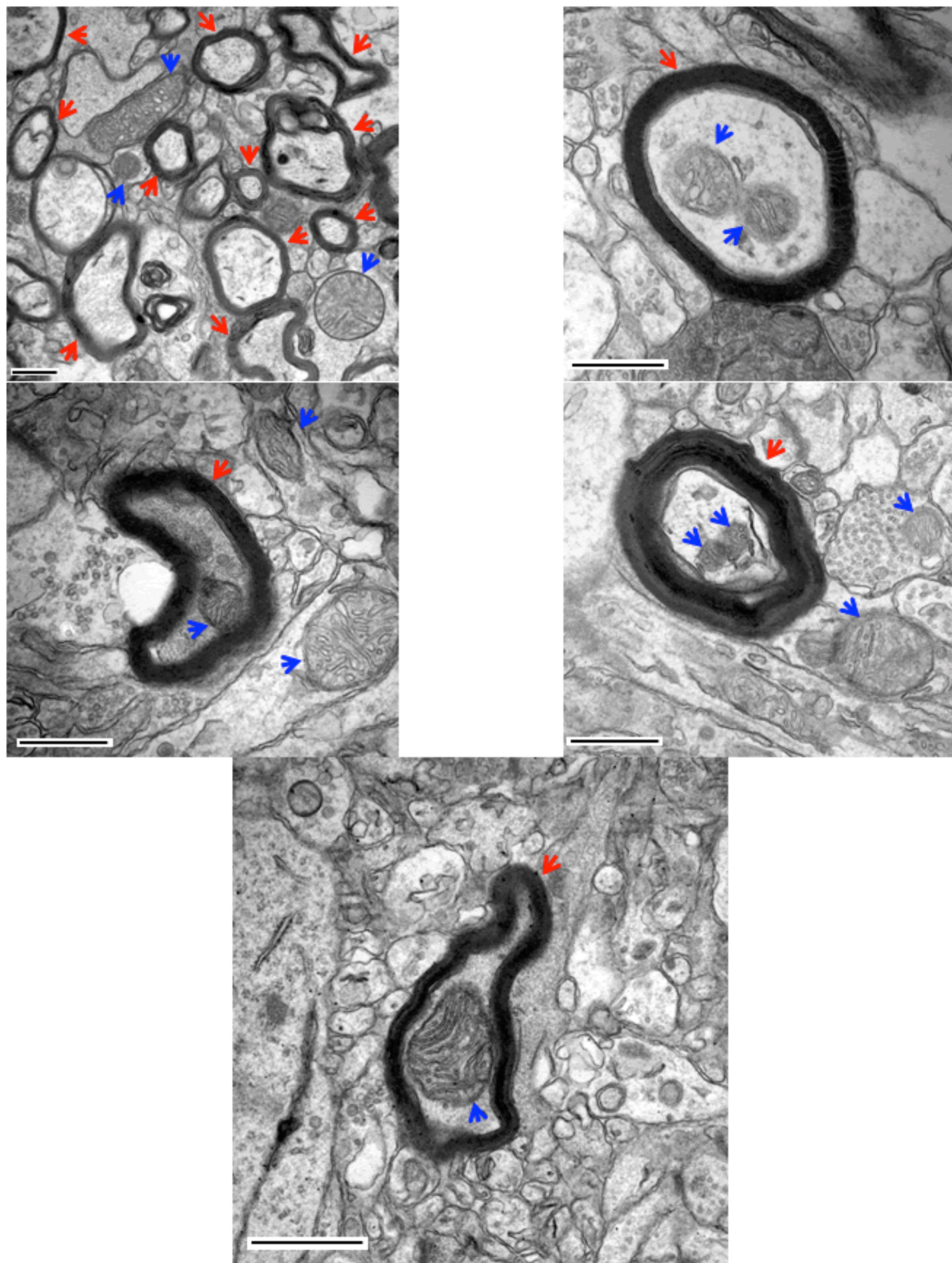


Figure S5

Foot Slip Assay in Wild Type Mice 8 Months After a Single Blast-Injury

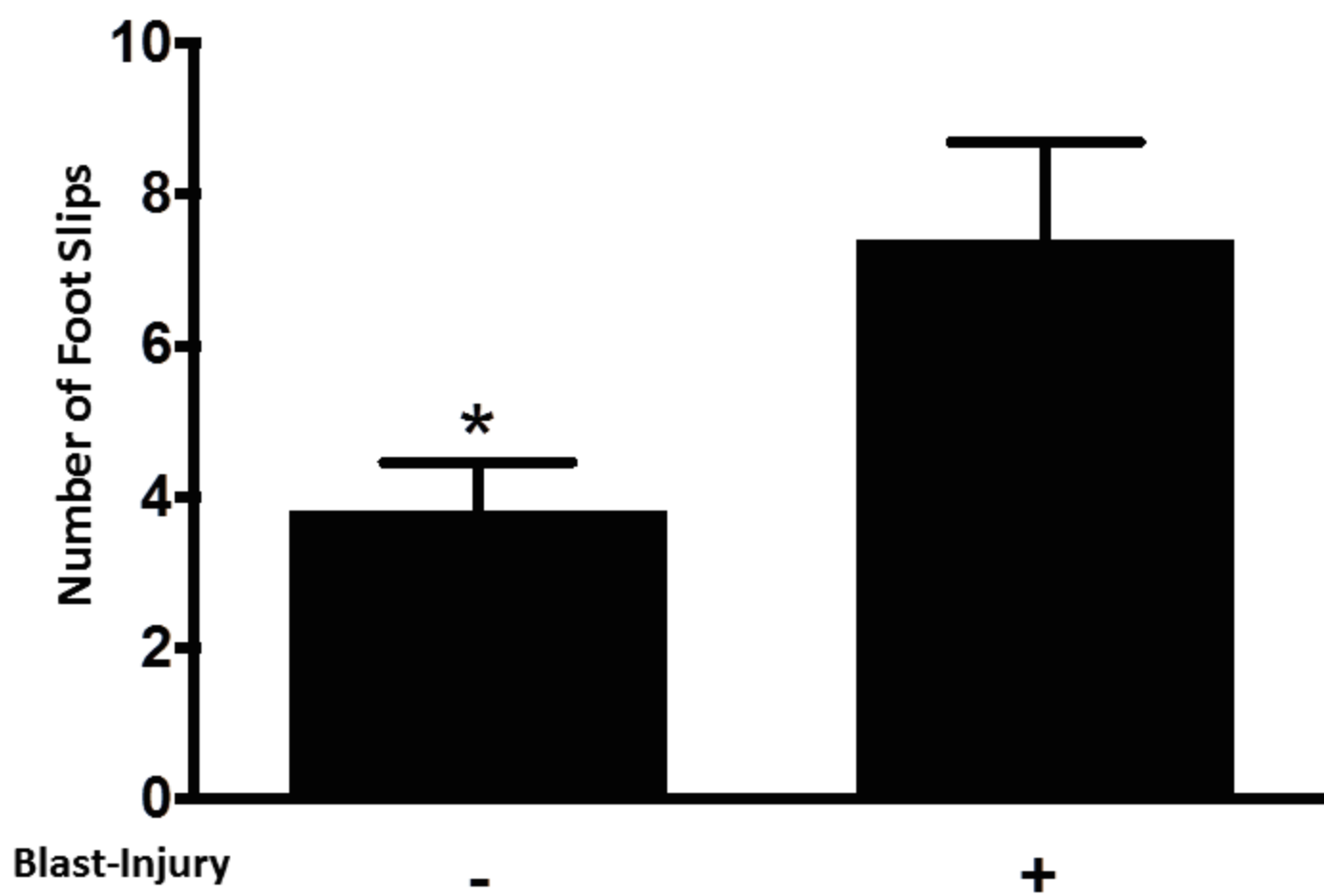


Figure S6A

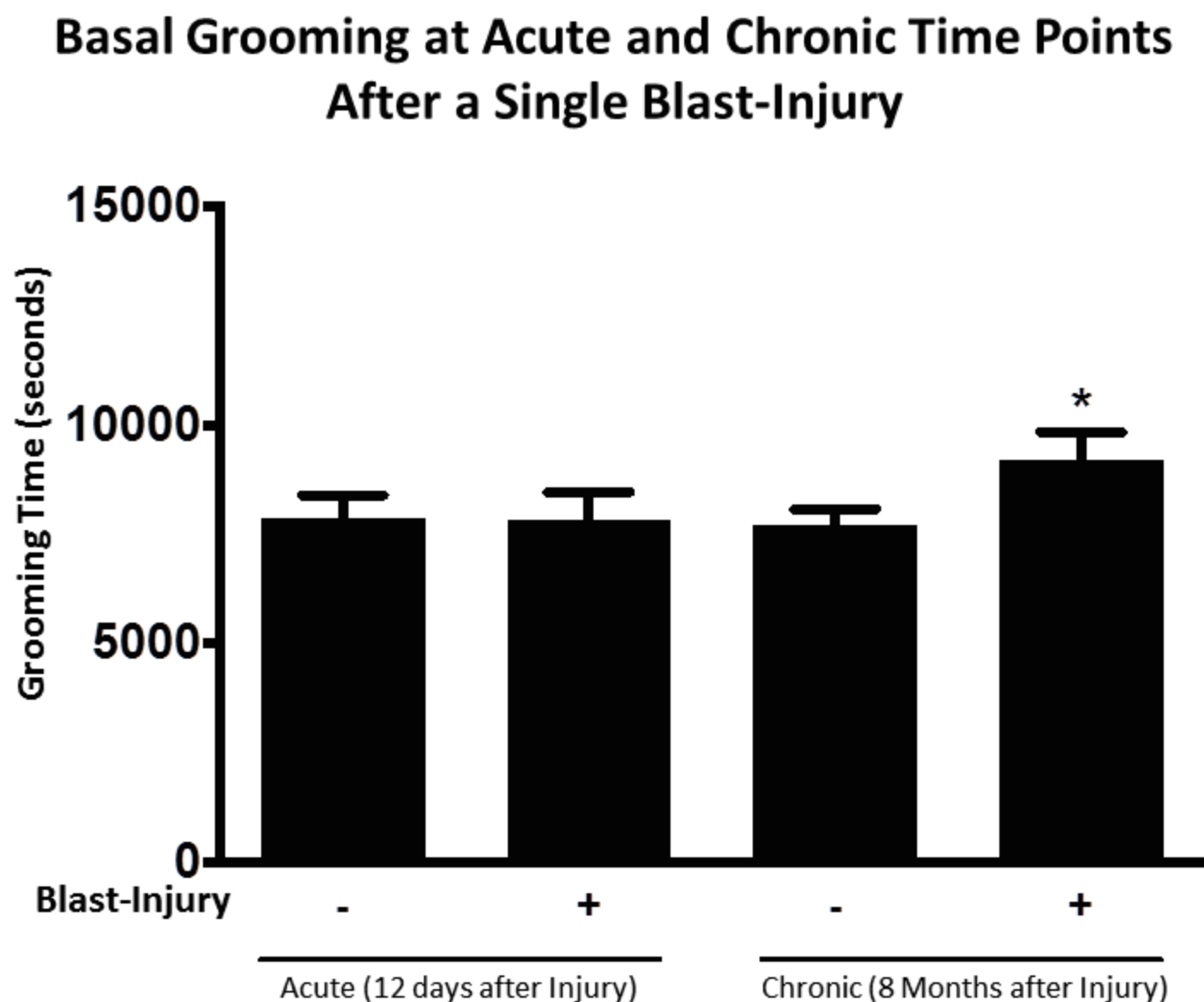
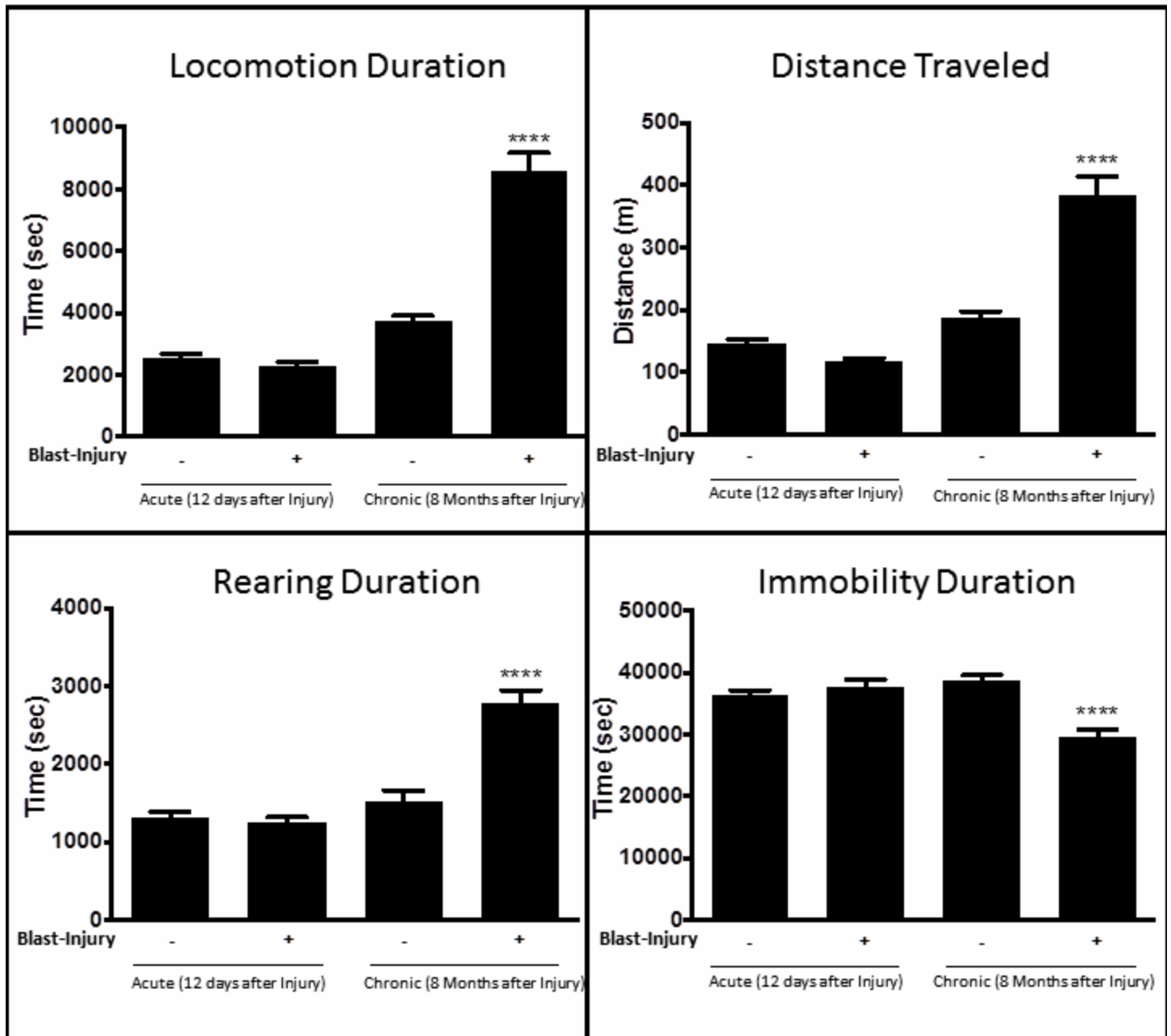


Figure S6B

Hyperactivity is Acquired at Chronic Time Point after a Single Blast-Injury



Supplemental Methods

Blood brain barrier (BBB) permeability assay. To analyze the permeability of the BBB, we used an Evan's blue dye (EBD) method modified from Uyama et al. (1988). EBD, which binds albumin, is incapable of crossing an intact blood-brain barrier. One hour prior to sacrifice, freshly prepared 2% EBD (Sigma) in phosphate-buffered saline (PBS) was administered at a 4 ml/kg dose via the retro-orbital venous sinus. Animals were sacrificed and perfused 6 hours, 24 hours, and 102 hours following blast-injury with cold PBS. Brains were frozen at -20 °C until all time points were complete to accurately compare each group. To quantify the extravasation of albumin-bound EBD in each brain, tissue was weighed and incubated for 30 minutes at room temperature in 50% trichloroacetic acid (TCA) in PBS at a 3:1 $\mu\text{l}/\text{mg}$ ratio. Samples were sonicated at 40% amplitude and centrifuged for 20 minutes at 10,000 rpm. Supernatants were transferred to new tubes and 100% ethanol was added in a 1:3 ratio. Fluorescence was measured using a SpectraMax M2^e (Molecular Devices) in 100 μl of samples plated on a 96-well plate at excitation wavelength of 620 nm and an emission wavelength of 680 nm.

Barnes Maze. The Barnes maze test assesses spatial learning and memory. It was conducted on a gray circular surface 91 cm in diameter with 20 holes 5 cm in diameter around the perimeter raised to a height of 90 cm (Stoelting Co.). The surface was brightly lit and open in order to motivate the test animal to learn the location of a dark escape chamber recessed under one of the 20 holes. The maze was placed inside a black circular curtain with four different visual cues (with different shapes and colors) for orientation to the permanent location of the escape chamber. Four days of training comprised of four trials per day were conducted for each animal. An area extending 4 cm from the escape hole in all directions was used as the target area for measurements (percent time in escape area, percent latency to escape and nose pokes). A probe trial was conducted on the subsequent day during which the escape chamber was removed and measurements were made to confirm the animal's memory based upon spatial cues. Measurements were made utilizing Anymaze video tracking software (Stoelting Co.), and analysis was conducted blind to treatment group.

Immunohistochemistry. Formaldehyde-perfused and fixed mouse cerebrum, brainstem and cerebellum were cryoprotected with 0.1 M phosphate buffer (PB, pH 7.4) containing 20% sucrose for 72 hours, and rapidly frozen in isopentane pre-cooled to -70°C with dry ice. All brains were stored in a freezer at -80°C before sectioning. Serial sections (40 μm) were cut coronally through the cerebrum, approximately from bregma 3.20 mm to bregma -5.02 mm and the brainstem and cerebellum, approximately from bregma -5.52 mm to bregma -6.96 mm (cf. the Mouse Brain in Stereotaxic Coordinates by Paxinos & Franklin, 1997). Every section in a series of 12 sections (interval: 480 μm) was collected separately. All sections were stored free-floating in FD sections storage solution (FD Neurotechnologies, Columbia, MD) at -20°C before further processing.

For hematoxylin & eosin (H&E) staining, sections were mounted on 1"x3" Superfrost Plus microscope slides and stained with FD hematoxylin & eosin (FD Neurotechnologies).

For silver staining, sections were collected in 0.1 M phosphate buffer (pH 7.4) containing 4% paraformaldehyde and fixed for 5 days at 4°C. Sections were then processed for the detection of neurodegeneration with FD NeuroSilver Kit II (FD Neurotechnologies) according to the manufacturer's instructions (for detailed procedures, cf. the manual of PK301, available at www.fdtypeurotech.com). Subsequently, all sections were mounted on slides, dehydrated in ethanol, cleared in xylene, and coverslipped with Permount (Fisher Scientific, Fair Lawn, NJ).

For NeuN- and GFAP- immunoreactivity, we first inactivated the endogenous peroxidase activity with 0.6% hydrogen peroxidase, and then sections were incubated free-floating for 43 hours at 4 °C in 0.01 M phosphate-buffered saline (PBS, pH 7.4) containing 1% normal blocking serum, 0.3% Triton X-100 (Sigma, St. Louis, MO) and either a biotin-conjugated monoclonal mouse anti-NeuN IgG (1:600; Millipore, Billerica, MA) or rat anti-GFAP IgG (1:10,000; Invitrogen, Carlsbad, CA). The immunoreaction product was visualized according to the avidin-biotin complex method with the Vectastin elite ABC kit (Vector Lab., Burlingame, CA). In brief, sections were incubated in PBS containing normal blocking serum, Triton-X and biotinylated rabbit anti-rat IgG (for GFAP) for 1 hour, and then in PBS containing avidin-biotinylated horseradish peroxidase complex for another hour. This was followed by incubation of sections for 6-10 minutes in 0.05 M Tris buffer (pH 7.2) containing 0.03% 3',3'-diaminobenzidine (Sigma) and 0.0075% H₂O₂ (Sigma). All steps were carried out at room temperature except indicated, and each step was followed by washes in PBS. After thorough rinses in distilled water, all sections were mounted on slides, dehydrated in ethanol, cleared in xylene, and coverslipped in Permount (Fisher Scientific, Fair Lawn, NJ). All images were taken with an Aperio ScanScope (Leica biosystems)

Quantification of immunohistochemistry: Optical densitometry for quantification procedures were modified from published methodology (Baldock and Poole et al. 1993). Images were captured with an upright microscope (Zeiss AxioImager.M2) equipped with a monochromatic digital camera (Zeiss AxioCam MRm Rev.3) and processed with the Zen imaging software (Zeiss 2012, Blue edition). The microscope light intensity and camera exposure were held constant. The operator outlined areas of interest around specific brain regions and recorded the intensity of light passing through the slide. Degenerating axons allowed less light to pass through the section due to their uptake of silver stain, so lower light intensity correlated with increased degeneration. The operator performing quantification was blinded to condition and treatment. This technique was verified to correlate with traditional measure of optical density of scanned tissues using NIH Image J, as described in the text.

Toluidine blue staining and transmission electron microscopy (TEM).

Mice were transcardially perfused with Karnovsky's fixative solution (2% formaldehyde, 2.5% glutaraldehyde, 0.2M sodium cacodylate buffer, 1mM CaCl₂, 2mM MgCl₂, and 42.8mM NaCl, pH 7.4) two weeks after either sham- or blast-Injury and with or without specified compound treatment. Harvested brains were incubated in Karnovsky's fixative solution overnight at 4 °C. Whole brains were cut in the horizontal plane (100µm) using a vibratome (Leica 1500). Sections that contained the hippocampus were selected, washed with 0.1M sodium cacodylate buffer and then post fixed with 1% osmium fixative for 1hr. After washing in 0.1M sodium cacodylate buffer, sections were dehydrated in a series of ethanol (50%, 75%, 95% and 100% ethanol) followed by embedding in EPON resin overnight at 65 °C. For toluidine blue staining, semithin sections (1µm) were cut with an ultramicrotome (Leica UC6) and stained with toluidine blue. Pictures were taken using an upright microscope (Zeiss Axio Imager.M2) with a color camera (AxioCam ICc5). For TEM, ultrathin sections (60nm) adjacent to the semithin sections were cut with an ultramicrotome, loaded onto a Formvar 200-mesh Ni grid, and counterstained with uranyl acetate and lead citrate. Specimens were examined using a JEOL JEM 1230 electron microscope with a Gatan UltraScan 1000 2k x 2k CCD camera. **See also Figure S4.**

Electrophysiology. Single-housed, naïve 7- to 9-week-old male C57BL/6J mice received intraperitoneal injections of P7C3-S243 (0.3, 3, or 30 mg/kg/day) or vehicle 24h following a single sham- or blast-Injury. On the tenth day after injury, coronal hippocampal slices (400 µm) were prepared, in accordance with the University of Iowa guidelines. Briefly, hippocampal slices were cut using a Vibratome 1000 Plus (Vibratome, St. Louis, MO) in ice-cold slicing buffer (in mM: 127 NaCl, 26 NaHCO₃, 1.2 KH₂PO₄, 1.9 KCl, 1.1 CaCl₂, 2 MgSO₄, 10 D-Glucose) bubbled with 95% O₂ and 5% CO₂. Slices were then transferred to a holding chamber containing oxygenated artificial cerebrospinal fluid (ACSF; in mM: 127 NaCl, 26 NaHCO₃, 1.2 KH₂PO₄, 1.9 KCl, 2.2 CaCl₂, 1 MgSO₄, 10 D-Glucose) for 30 min at 34 °C and for another 30 min at 22 °C for recovery, and then transferred to a submersion recording chamber continually perfused with 32 °C oxygenated ACSF (rate: 2 ml/min). Slices were equilibrated for at least 15 min before each recording.

ACSF-filled glass electrodes (resistance <1 MΩ) were positioned in the stratum radiatum of area CA1 for extracellular recording. Synaptic responses were evoked by stimulating Schaffer collaterals with 0.2 ms pulses once every 15 s. The stimulation intensity was systematically increased to determine the maximal field excitatory post-synaptic potential (fEPSP) slope and then adjusted to yield 40-60% of the maximal (fEPSP) slope. Experiments with maximal fEPSPs of less than 0.5 mV, with large fiber volleys, or with substantial changes in the fiber volley during recording were rejected. LTP was induced by 12TBS (12 bursts, each of 4 pulses at 100 Hz).

Field EPSPs were recorded (AxoClamp 900A amplifier, Axon Instruments, Foster City, CA), filtered at 1 kHz, digitized at 10 kHz (Axon Digidata 1440), and stored for

off-line analysis (Clampfit 10). Initial slopes of fEPSPs were expressed as percentages of baseline averages. In summary graphs, each point represents the average of 4 consecutive responses. Time-matched, normalized data were averaged across experiments.

IL-1 pathway examination with RT² Profiler PCR Array. 1µg total RNA (from whole hippocampus) was used for cDNA synthesis for 2 hours post TBI samples via RT² first strand kit (SAbioscience 330401). 2ug total RNA (from whole hippocampus) was used for cDNA synthesis for 24 hours post TBI samples. RT² syber green mastermix (SAbioscience 330522) and RT² profiler PCR array (Inflammatory Response & Autoimmunity PCR Array, Cat. no. PAMM-077Z, Qiagen) were used for real time PCR following manufacturer's instruction. Housekeeping genes used as endogenous controls included ACTB, B2M, GAPDH, GUSB, HSP90AB1.

Foot slip assay. We used standard procedures described by Luong et. al. (2011) to measure motor balance coordination. During the training period, mice were trained to cross the 80cm beam to enter a black box with nesting material 3 times a day over 2 consecutive days. Mice were then sham- or blast-injured on the next day. 24hrs after injury, daily administration with (-)-P7C3-S243 or vehicle was initiated. Animals were then tested 7 and 28 days after injury. Mice performance was videotaped during the test and foot slips were analyzed by an observer blind to condition and treatment group.

LABORAS assay. LABORAS (Metris) is a system that uses a carbon fiber plate to detect behavior-specific vibration patterns created by animals. Various behavioral parameters are determined by LABORAS software processing of the vibration pattern. Data were collected uninterrupted over a 24-h period, enabling comprehensive quantification of basal grooming time and locomotor activity in the home cage environment throughout the light-dark cycle. Before data collection, test animals were acclimated in the test room for 1 wk. Then, test animals were placed in a standard cage atop the carbon fiber platforms. Vibrations were recorded for 24 h, and then the animals were removed. Vibration data were processed via LABORAS 2 software.

References:

Baldock, R.A., and Poole, I. (1993). Video camera calibration for optical densitometry. *J Microsc* 172, 49-54.

Figure S1. Protective Efficacy of Immediate Administration of P7C3-S243, Dynamics of Blood-Brain-Barrier Integrity after Blast-Injury, and Experimental Design of Subsequent Experiments, Related to Figure 1. **(A)** Administration of P7C3-A20 or P7C3-S243 (10 mg/kg/d administered IP in divided daily doses for 11 days), within 30-60 seconds after blast-mediated TBI, preserves hippocampal-dependent spatial memory in the Barnes maze 11 days after injury. Animals subjected to sham-injury and administered vehicle, or the same doses of P7C3-A20 or P7C3-S243, spent $\approx 60\%$ of their time in the escape quadrant, in contrast to blast-injured vehicle controls, which spent $\approx 20\%$ of their time in the escape quadrant. This same treatment with P7C3-A20 or P7C3-S243 immediately after blast-injury rescued memory to normal levels in sham-injured mice. In both blast-injured and sham-injured groups, treatment with (-)-P7C3-S243 showed a nonsignificant trend in increasing time spent in the escape quadrant. 12 male C57/Bl6 mice aged 12-14 weeks were tested per group, and data was collected and scored in an automated manner blind to treatment group. Significance was determined by 2 way ANOVA with Bonferroni post-hoc analysis. p-value labeled as $* < 0.05$, $** < 0.01$, $*** < 0.001$, compared to blast-injured animals treated with vehicle. **(B)** Blood-brain-barrier permeability is compromised at 6 hours after blast injury, and returns to normal 24 hours after injury. Daily treatment with P7C3-S243 (10 mg/kg/d) for four days does not affect blood brain barrier permeability. 5 male C57/Bl6 mice aged 12-14 weeks were tested per group. Significance was measured using two way ANOVA. Data are represented as mean \pm SEM. p-value labeled as $**** < 0.0001$, compared to uninjured animals treated with vehicle. **(C)** Schematic of experimental design of subsequent experiments.

Figure S2. Target Entry, Quadrant Time, Speed, Distance Traveled, and Learning in Veh and P7C3-S243 Treated Mice After Blast-Injury, and Persistent Deficits in Learning and Memory in Untreated Mice After Blast-Injury in the Barnes Maze, Related to Figure 1. **(A)** Daily IP administration of P7C3-S243 for 11 days in divided daily doses as indicated dose-dependently preserved performance in the probe test of the Barnes maze in blast-injured mice, as measured by the percent target entry. This metric is defined as the number of times a mouse pokes its nose into the correct hole out of the total number of times it pokes its nose into any hole. Treatment with an intermediate dose (3 mg/kg/d) of the active (-)-P7C3-S243 enantiomer preserved normal performance in this measure to the level displayed by sham-injured mice. By contrast, mice treated with the less active (+)-P7C3-S243 enantiomer showed the same deficit as blast-injured mice treated with vehicle. **(B)** Daily administration of P7C3-S243 was initiated at progressively later time periods after injury, in order to define the window of therapeutic efficacy. Whereas both 3 and 30 mg/kg/d doses preserved a normal percent target entry when treatment was initiated 24 hours after injury, only the higher dose was significantly protective when daily treatment was initiated at 36 hours. When treatment was initiated 48 hours after injury, no protective efficacy was noted at any dose. **(C)** Oral (PO) administration of the highly active (-)-P7C3-S243 enantiomer showed potent preservation of percent target entry at 3, 10 and 30 mg/kg/day doses. **(D)** Daily IP administration of racemic

P7C3-S243 for 11 days in divided daily doses as indicated dose-dependently preserved performance in the probe test of the Barnes maze in blast-injured mice, as measured by the percent quadrant time. This metric is defined as the percentage of time the mouse spends in the quadrant containing the escape hole. Treatment with an intermediate dose (3 mg/kg/d) of the active (-)-P7C3-S243 enantiomer completely preserved normal performance in this assay to the level displayed by sham-injured mice. Mice treated with the less active (+)-P7C3-S243 enantiomer showed some protection at the margin of statistical significance, but not to the degree effected by equivalent doses of racemic P7C3-S243 or (-)-P7C3-S243. **(E)** Daily administration of racemic P7C3-S243 was initiated at progressively later time periods after injury, in order to define a window of therapeutic efficacy. Whereas 3 and 30 mg/kg/d doses preserved a normal percent quadrant time when treatment was initiated 24 hours after injury, only the higher dose was significantly protective when daily treatment was initiated 36 hours after injury. When treatment was initiated 48 hours after injury, no protective efficacy in this assay was noted at any dose of racemic P7C3-S243. **(F)** Oral (PO) administration of the highly active (-)-P7C3-S243 enantiomer showed potent preservation of percent quadrant time at 3, 10 and 30 mg/kg/day doses. **(G)** Speed did not differ as a function of blast-injury or treatment initiated 24 hours after injury. **(H)** Speed did not differ as a function of compound administered (IP) 36 or 48 hours after injury. **(I)** Speed did not differ as a function of oral (PO) administration of compound to blast-injured animals. **(J)** Distance traveled did not differ as a function of blast-injury or treatment (IP) initiated 24 hours after injury. **(K)** Distance traveled did not differ as a function of compound administered (IP) 36 or 48 hours after injury. **(L)** Distance traveled did not differ as a function of oral (PO) administration of compound to blast-injured animals. **(M)** Learning was assessed as the percent latency to escape, defined as the percentage of time the mouse took to enter the escape hole on day 4 out of the time that it required on day 1. Mice subjected to blast-mediated TBI and then treated with vehicle, 0.3 mg/kg/day P7C3-S243, or 3 mg/kg/day (+)-P7C3-S243 learned significantly more poorly than did sham-injured mice. When treatment with 1, 3, 10 or 30 mg/kg/day P7C3-S243 (IP), or 3 mg/kg/day (-)-P7C3-S243 (IP), was initiated 24 hours after injury, however, all groups learned the task equally well. **(N)** Daily administration of P7C3-S243 was initiated at progressively later time periods after injury, in order to define a window of therapeutic efficacy. Whereas 3 and 30 mg/kg/day doses preserved a normal percent latency to escape when treatment was initiated 24 hours after injury, only the higher dose was protective when treatment was initiated at 36 hours. However, some protective efficacy was also seen at the lower dose of 3 mg/kg/day (IP) when treatment was initiated at this time point. When treatment was initiated 48 hours after injury, protective efficacy was noted at 30 mg/kg/day (IP) P7C3-S243. **(O)** Oral (PO) administration of the highly active (-)-P7C3-S243 enantiomer preserved of normal percent latency to escape at 1, 3, 10 and 30 mg/kg/day doses. For **(A–O)**, every group shown consisted of 25 male C57/Bl6 mice, aged 12-14 weeks, and data was collected and scored in an automated manner blind to treatment group. Data are represented as mean \pm SEM. Significance was determined by two-way ANOVA with Bonferroni post-hoc analysis. p-value labeled as * <0.05 , ** <0.01 , *** <0.001 , and **** <0.0001 compared to blast-injured animals treated with vehicle.

(P) After blast-injury, both sham groups, regardless of the amount of time after injury, spent ~40% of total probe trial time in the target area. Blast injured groups, by contrast spent less than 20% total time in target area. Blast-injury causes a similar decrement in performance in the **(Q)** % target entry and **(R)** % time spent in the escape quadrant at both acute and chronic time points after injury. **(S)** Speed during the probe trial was measured and was consistent between sham and blast-injured mice in both acute and chronic groups. **(T)** Total distance traveled during the probe trial was no different when mice were tested at 2 months of age. However when mice were tested at the chronic time point of eight months after injury, the blast-injured group traveled a greater distance than sham animals. **(U)** Sham animals had a decreased latency to escape compared to blast-injured animals at both 2 and 10 month of age, though older sham mice in the chronic group learned more slowly than the corresponding younger mice in the acute sham group. The acute group consisted of 25 male C57/Bl6 mice, and the chronic group consisted of 22 sham C57/Bl6 mice and 21 blast-injured C57/Bl6 mice. Data was collected and scored in an automated manner blind to treatment group. Significance was determined by two-tailed students' T-Test. p-value labeled as * <0.05 , ** <0.01 , *** <0.001 , and **** <0.0001 compared to blast-injured animals.

Figure S3. Histologic quantification of Tissue Damage After Blast-Injury, Related to Figure 3. **(A)** Optical densitometry of silver-stained CA1 stratum radiatum by NIH Image J from all animals in each group was used to quantify the protective effect by identifying degenerating axons in brain tissue. Every group shown consisted of the identical sections analyzed in Figure 3, from 5 male C57/Bl6 mice, aged 12-14 weeks. Data was collected and scored blind to treatment group. Significance was determined by 1 way ANOVA with Bonferroni post-hoc analysis. p-value labeled as * <0.05 , ** <0.01 , *** <0.001 , and **** <0.0001 compared to blast-injured animals treated with vehicle. **(B)** Shown at 80X magnification for clarity of morphology (scale bar = 5 μ M) is prominent silver staining of degenerating axons in CA1, corpus callosum, thalamus, cortex, olfactory bulb, striatum, dentate gyrus and cerebellum of blast-injured animals treated with vehicle, low dose (0.3 mg/kg/day) P7C3-S243, or intermediate dose (3 mg/kg/day) of the less active enantiomer (+)-P7C3-S243. Silver staining shows no evidence of axonal degeneration in sham-injured mice treated with vehicle, or in blast-injured mice treated with 3 or 30 mg/kg/day doses of P7C3-S243. Blast-injured mice were also protected from axonal degeneration by treatment with 3 mg/kg/day dose of the highly active enantiomer (-)-P7C3-S243. No axonal degeneration was observed in the hypothalamus as a result of blast-injury. Images shown are representative of brain slices from 5 animals in each group. **(C)** Same as **(B)**, with lower power (40X, scale bar = 2.5 μ M) images showing breadth of axonal staining. **(D)** Optical densitometry of light transmitted through the indicated silver stained regions from all animals in each group was used to quantify the protective effect. The specific tissue area was manually delineated, and signal was quantified for 18 sections for each of the 5 animals, spaced 480 μ M apart. Here, a greater value indicates that more light was able to pass unimpeded through the section by virtue of less silver staining, which indicates less axonal degeneration. Data are represented as mean \pm SEM. P-value * <0.05 , * <0.01 , ** <0.001 determined by-two

way ANOVA with Bonferroni post-hoc analysis. **(E)** Immunohistochemical staining for NeuN shows no evidence of frank neuronal cell loss after blast-mediated TBI in CA1, corpus callosum, thalamus, cortex, olfactory bulb, striatum, or hypothalamus. Images shown are representative of brain slices from 5 animals in each group, directly adjacent to those shown in Figure S7. Scale bar = 5µM. **(F)** NeuN-stained cells were quantified for 18 sections for each of the 5 animals, spaced 480 µM apart. Data are represented as mean ± SEM. No significant differences between groups were noted by two-way ANOVA with Bonferroni post-hoc analysis. **(G)** Hematoxylin and eosin (H&E) staining shows no evidence of cell loss after blast-mediated TBI in CA1, corpus callosum, thalamus, cortex, olfactory bulb, striatum, or hypothalamus. Images shown are representative of brain slices from 5 animals in each group, directly adjacent to those shown in Figure S7. Scale bar = 5µM. **(H)** H&E staining in 18 sections for each of the 5 animals, spaced 480 µM apart, was quantified. Data are represented as mean ± SEM. No significant differences between groups were noted by two-way ANOVA with Bonferroni post-hoc analysis. **(I)** Immunohistochemical staining for glial fibrillary acidic protein (GFAP) shows no elevation after blast-injury, thus providing no evidence of neuroinflammation. Images shown are representative of brain slices from 5 animals in each group, directly adjacent to those shown in **(G)**.

Figure S4. Transmission Electron Microscopy and Toluidine Blue Staining, Related to Figure 4. **(A)** This diagram shows the methodology of tissue processing for toluidine blue and transmission electron microscopy (TEM). Both hemispheres of the hippocampus (red rectangles) were used for evaluation of pathology. **(B)** Toluidine blue staining showed that blast-injury vehicle-treated mice accumulate chromatolytic and pyknotic neurons in the CA1 region, and that initiation of daily oral treatment of blast-injured mice with (-)-P7C3-S243 prevents this pathology. Pictures shown are representative of 4 animals for each condition, and are from different animals than the pictures shown in figure 4. Scale bar = 20µm **(C)** TEM showing protection against myelin degeneration (red arrows) and mitochondrial swelling (blue arrows) in stratum radiatum of blast-injury mice treated with 30 mg/kg/day (-)-P7C3-S243. These pictures are from different animals than the pictures in Figure 4 (scale bar = 500nm). **(D)** TEM visualization of hippocampal axonal and mitochondrial structures 2 weeks after sham-injury in mice administered vehicle, showing normal myelin sheath (red arrows), along with intact outer membrane and internal cristae structures within mitochondria (blue arrows) in the hippocampus stratum radiatum (scale bars = 500nm). **(E)** TEM visualization of hippocampal axonal and mitochondrial structures 2 weeks after sham-injury in mice treated orally with 30 mg/kg/day of (-)-P7C3-S243, showing normal myelin sheath (red arrows), along with intact outer membrane and internal cristae structures within mitochondria (blue arrows) in the hippocampus stratum radiatum (scale bars = 500nm). **(F)** TEM visualization of hippocampal axonal and mitochondrial pathology 2 weeks after blast-injury in mice receiving vehicle, showing degeneration of myelin sheath (red arrows), along with abnormal outer membrane and internal cristae structures within mitochondria (blue arrows) in the hippocampus stratum radiatum (scale bars, 500nm). **(G)** TEM visualization of hippocampal axonal and mitochondrial structures 2 weeks after

blast-injury in mice treated orally with 0.3 mg/kg/day of (-)-P7C3-S243, showing no preservation of myelin sheath (red arrows), along with abnormal outer membrane and internal cristae structures within mitochondria (blue arrows) in the hippocampus stratum radiatum (scale bars, 500nm). **(H)** TEM visualization of hippocampal axonal and mitochondrial structures 2 weeks after blast-injury in mice treated orally with 3 mg/kg/day of (-)-P7C3-S243, showing preservation of myelin sheath (red arrows), along with very minimal outer membrane and internal cristae structures within mitochondria (blue arrows) in the hippocampus stratum radiatum (scale bars = 500nm). **(I)** TEM visualization of hippocampal axonal and mitochondrial structures 2 weeks after blast-injury in mice treated orally with 30 mg/kg/day of (-)-P7C3-S243, showing preservation of myelin sheath (red arrows), along with normal outer membrane and internal cristae structures within mitochondria (blue arrows) in the hippocampus stratum radiatum (scale bars = 500nm).

Figure S5. Chronic Motor Deficits after Blast Injury, related to Figure 5. Eight months after a single blast-injury, mice display twice as many foot slips as sham-injury control mice. Sham animals consisted of 22 male C57/Bl6 mice, and blast-injured animals consisted of 21 male C57Bl6 mice. Data was collected and scored by an observer blinded to identity of the group. Significance was determined by two-tailed students' T-Test. p-value labeled as $* < 0.05$ compared to blast-injured animals.

Figure S6. Acquisition of Chronic Neuropsychiatric Deficits Related to Anxiety in Untreated Mice after Blast-Injury, related to Figure 5. **(A)** Basal grooming is elevated chronically after a single blast-injury. Grooming behavior was quantified with LABORAS® equipment. At the acute time point, there was no difference in 24 hour grooming time between blast-injury and sham-injury groups. Eight months after blast-injury, however, mice showed acquisition of elevated grooming time, relative to sham-injury mice. Both blast-injury and sham-injury acute groups consisted of 25 male C57/Bl6 mice, and the chronic groups consisted of 22 sham C57/Bl6 mice and 21 blast-injured C57/Bl6 mice. Data was collected and scored in an automated manner blind to treatment group. Significance was determined by two-tailed students' T-Test. p-value labeled as $* < 0.05$ compared to blast-injured animals. **(B)** Hyperactivity is acquired chronically after a single blast-injury. 24 hr activity was monitored using LABORAS® equipment. 12 days after blast-injury, mice did not exhibit any difference in locomotion time. However, eight months after injury, locomotion was increased by 2.5 fold in the blast injured group relative to sham controls. 12 days after blast-injury, distance traveled in the course of 24hrs was not different between sham and blast-injured groups. Eight months after injury, however, blast-injured mice exhibited a two-fold increase in distance traveled compared to sham controls. 12 days after blast-injury, there was no difference in rearing activity between blast-injured and sham groups. However, eight months after injury, blast-injured mice exhibited ~3 fold increase in rearing time over sham controls. 12 days after blast-injury, the time spent immobile was not different between blast-injured and sham groups. However, eight months after blast injury, the blast-injured group exhibited a 25% decrease in immobile time relative

to sham controls. Both acute groups consisted of 25 male C57/Bl6 mice, and the chronic groups consisted of 22 sham C57/Bl6 mice and 21 blast-injured C57/Bl6 mice. Data was collected and scored in an automated manner blind to treatment group. Significance was determined by two-tailed students' T-Test. p-value labeled as ****<0.0001 compared to blast-injured animals.